Modelling of regenerator units in fluid catalytic cracking processes

Miguel André Freire de Almeida

Thesis to obtain the Master of Science Degree in

Chemical Engineering

Supervisors: Prof. Dr. Carla Isabel Costa Pinheiro

Dr. Stepan Spatenka

Examination Committee

Chairperson:	Prof. Dr. José Manuel Madeira Lopes
Supervisor:	Prof. Dr. Carla Isabel Costa Pinheiro
Member of the committee:	Prof. Dr. Rui Manuel Gouveia Filipe

July 2016

Acknowledgements

First of all, I would like to thank Prof. Dr. Carla Pinheiro, Dr. Stepan Spatenka and Vasco Manaças for supervising this work and advising me at every step. I would also like to thank everyone at Process Systems Enterprise for the opportunity for developing this work and for the great working environment that exists there.

I would also like to thank my housemates and fellow interns at PSE for the seven months that the internship lasted.

Lastly, I would like to thank all of my family and friends for all of the support given to me during this internship and the development of this work.

Abstract

Fluid Catalytic Cracking (FCC) is a very important process present in many refineries around the world, as it can transform heavy fractions of petroleum, with low value, to gasoline and other products with higher value.

In this work, a working model for the regenerator of a fluid catalytic cracking unit is developed based on the generalised fluidised bed reactor model by Abba. This model is substantially more complex than other regenerator models found in literature. The model is used to test several common simplifying assumptions found in other models from literature. A sensitivity analysis is also performed with the model.

The model is subject to a limited validation with plant and simulation data from literature.

The main results of the studies performed with the regenerator model include: the necessity of considering the combustion of hydrogen in the regenerator modelling and the confirmation of the catalyst flowrate and air flowrate as good manipulated variables for controlling the regenerator. The inclusion of dispersion in the reactor model is shown to be unnecessary, although further validation is required.

Keywords: FCC, regenerator, modelling, gPROMS, sensitivity analysis

Resumo

O cracking catalítico em leito fluidizado (FCC) é um processo muito importante presente em muitas refinarias em todo o mundo, dado que consegue transformar frações pesadas do petróleo, com baixo valor, em gasolina e outros produtos de valor mais elevado.

Neste trabalho, um modelo funcional do regenerador de uma unidade de FCC é desenvolvido com base no modelo do reator em leito fluidizado generalizado de Abba. Este modelo é substancialmente mais complexo do que outros modelos encontrados na literatura. O modelo é usado para testar várias hipóteses simplificativas de modelos de regenerador encontrados na literatura. É também realizada uma análise de sensibilidade.

O modelo foi sujeito a uma validação limitada com dados de fábrica e de simulação encontrados na literatura.

Os resultados principais dos estudos realizados com o modelo do regenerador incluem: a necessidade de considerar a combustão de hidrogénio na modelação do regenerador e a confirmação de que o caudal de catalisador e o caudal de ar são boas variáveis manipuladas para o controlo do regenerador. É também mostrado que a inclusão de dispersão no modelo do reator é desnecessária; contudo são necessários mais dados de validação para confirmar esta conclusão.

Palavras-chave: FCC, regenerador, modelação, gPROMS, análise de sensibilidade

Table of Contents

Index of Figures

Index of Tables

Glossary

Abbreviations

GFBR	Generalised fluidised bed reactor
CCR	Conradson Carbon Residue
CFD	Computational Fluid Dynamics
CST	Continuous stirred tank
CSTR	Continuous stirred tank reactor
FCC	Fluid catalytic cracking
FCCU	Fluid catalytic cracking unit
gML	gPROMS Model Libraries
gPROMS	general PROcess Modelling System
HCO	Heavy cycle oil
LCO	Light cycle oil
LPG	Liquefied petroleum gas
PFR	Plug flow reactor
PML	Process Model Libraries
RFCC	Residue fluid catalytic cracking
VGO	Vacuum gas oil

Variables

A_R Regenerator cross sections area (m^2)

C_{ik} Molar concentration of species *k* in phase *i* (mol/m^3)

C_{p_j} Specific heat capacity (J/kg/K)

D_{zi} Axial dispersion in phase *i* (m^2/s)

F_c Mass flowrate of catalyst particles (kg/s)

h_g Specific mass enthalpy of the gas phase (J/kg)

k_e Effective thermal conductivity of bed solids ($J/m^3/s$)

$k_{LH}a_I$ Volumetric mass transfer coefficient (1/s)

L_d Height of the dense bed (m)

L_f Height of the freeboard (m)

MW_{ck} Molar mass of coke (kg/mol)

r_{cik} Molar reaction rate of component *k* of coke in phase *i* (mol/kg/s)

r_{gik} Molar reaction rate of component *k* in phase *i* of the reactions in the gas phase ($mol/m^3/s$)

r_{sik} Molar reaction rate of component *k* in phase *i* of the reactions in the solids phase (mol/kg/s)

T_d Temperature in the dense bed (K)

T_f Temperature in the freeboard (K)

U_i Superficial velocity in phase *i* (m/s)

Y_k Mass ratio of component *k* of coke in the catalyst particles (kg/kg)

z_d Height coordinate in the dense bed (m)

z_f Height coordinate in the freeboard (m)

ε_i Void fraction in phase *i* (m^3/m^3)

ϕ_i Solid fraction in phase *i* (m^3/m^3)

Ψ_i Phase fraction of phase *i* in the dense bed (m^3/m^3)

ρ_i Gas density in phase *i* (kg/m^3)

Subscripts

i Can be L for the low density phase in the dense bed or H for the high density phase. When absent represents the variable for the whole dense bed or freeboard

in Value at the inlet to the regenerator

out Value at the outlet to the regenerator

j Can be p for the catalyst particles or g for the gas phase

1 Introduction

1.1 Motivation

Fluid catalytic cracking is a technology with more than 70 years. It was designed to continuously crack heavy fractions of petroleum, having replaced other cyclic processes used previously. [1]

FCC is mainly used to crack vacuum gas oil and other heavy fractions of petroleum. The main product that is desired from the FCC is gasoline, which can constitute about 60% of the gasoline pool in a refinery. [2] Figure 1.1 represents a typical refinery and shows where and how the FCCU is connected to the remaining processes of a refinery.

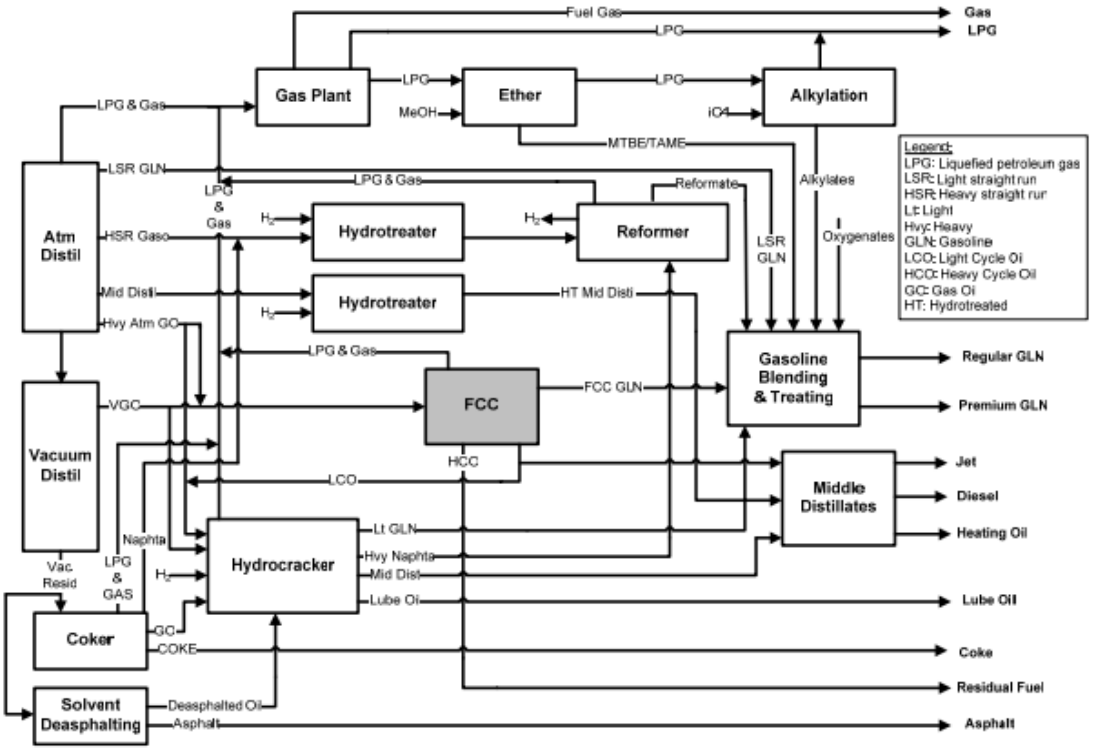

Figure 1.1 – Diagram of a refinery evidencing the location of the FCC unit. [3]

Being such a relevant process to a refinery, having an accurate model of a fluid catalytic cracking unit is important, to be able to test and simulate several scenarios to achieve the best operating conditions for the FCC without interrupting its operation. Due to the size and importance of the FCC to a refinery, even an improvement of 1% in its operation justifies the investment in producing such a model.

As such, the objective of this work is the development of a model of an FCCU regenerator, as accurate as possible and significantly more complex and complete than others found in literature, to be included in a library of reusable models to be interfaced with other models to create full FCCU processes. Another objective is to perform a sensitivity analysis on a number of key variables of the regenerator.

1.2 Thesis outline

This thesis is organised as follows:

- Chapter 1 presents the introduction and objectives of the thesis.
- Chapter 2 includes a literature review of the FCC and published models.
- Chapter 3 presents the work done in developing the regenerator model.
- Chapter 4 presents and discusses the results of the several simulations and sensitivity analysis done with the developed model.
- Chapter 5 presents some conclusions and suggestions for future work.

2 Background

This chapter presents the necessary background to comprehend the work developed in the rest of this thesis. It includes an explanation of the Fluid Catalytic Cracking (FCC) process and how a typical unit operates. It also includes possible modelling approaches to modelling a Fluid Catalytic Cracking Unit (FCCU) and a summary review of the models found in literature.

2.1 Fluid Catalytic Cracking

Fluid catalytic cracking is a process present in a majority of refineries [1], to process heavier fractions from the crude distillation, usually vacuum gas oil (VGO), to produce lighter fractions, mainly gasoline [2]. This process occurs in a pair of reactors: a riser, where the feed is injected with the catalyst and the cracking reaction occurs, and the regenerator, where the deactivated catalyst is regenerated by burning of the deposited coke. Figure 2.1 represents a simplified diagram of a FCCU with its main components identified. The entire process is in heat integration, with the heat released in the regeneration of the catalyst providing the energy necessary for the cracking reactions in the riser. [1], [4]

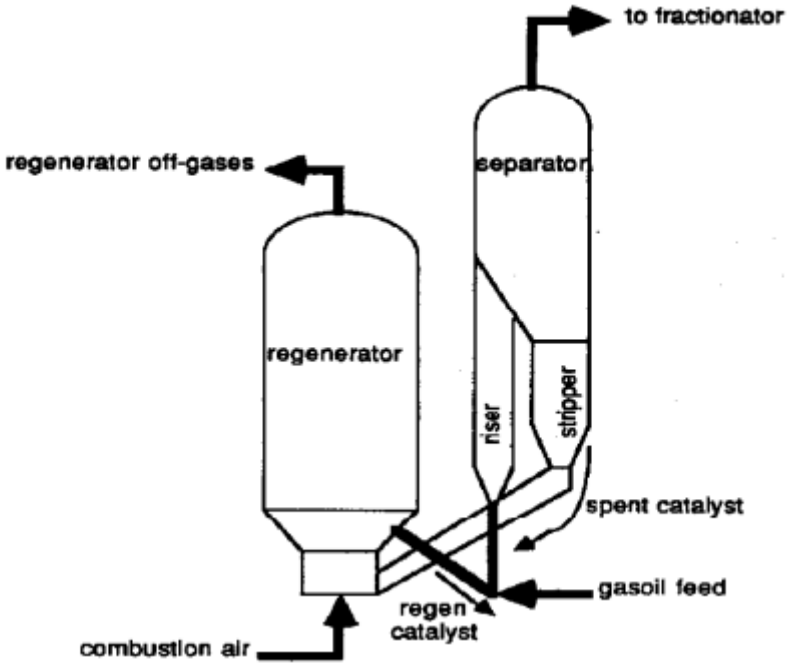

Figure 2.1 – Diagram of a fluid catalytic cracking unit. [5]

The feeds usually used in FCC are composed mainly of vacuum gas oil (VGO), but can also include atmospheric residue, or other heavier fractions of petroleum, to be also cracked. [2] Some specialized FCCU can also process residue directly [6], by being prepared to handle higher quantities of coke that those feeds produce.

Inside the riser, the feed is cracked by the catalyst, forming smaller hydrocarbons, but also coke, a high molecular weight, polyaromatic type of molecule. The coke is deposited on the

catalyst particles, where it will be burnt off in the regenerator, releasing the energy necessary for the cracking reactions, which are overall endothermic. [3]

Besides coke, the main products of the cracking reactions are [3]:

- Dry gas (C1-C2)
- Liquefied Petroleum Gas (LPG) (C3-C4)
- Gasoline (C5-221 ºC)
- Light Cycle Oil (LCO)
- Heavy Cycle Oil (HCO)
- Slurry/decant oil

The gasoline produced from FCC usually amounts to about 60% of the gasoline pool of a refinery.

The catalysts used in the FCC are zeolite based, with several other components and additives, and in the form of a small powder. The main components in the catalyst are: the zeolite, usually Y zeolite; amorphous alumina, that also has some cracking ability; a clay filler, to dilute the catalytic activity, function as a heat sink and provide mechanical resistance; and a binder to keep all of the components in the catalyst particles together. [3]

Some additives can also be added for specialized functions. These functions include [7]:

- Alter the FCC yields, such as adding ZSM-5 to increase the production of light olefins
- Promote the combustion of CO to CO2 in the regenerator
- SO_x and NO_x reducers
- Metal traps, to prevent the permanent deactivation of the catalyst by Ni, V and other metals.

The design of fluid catalytic cracking units falls in two categories, illustrated in Figure 2.2: the side-by-side and the stacked configuration. In the side-by-side configuration, the regenerator and the riser with the stripper on top are placed one next to the other. In the stacked configuration, the riser runs alongside the regenerator and terminates in a stripper that is placed on top of the regenerator.

2.2 FCC Process Description

The FCC process starts with the injection of the feed, usually VGO, into the riser. It is injected with special nozzles to create small droplets. The feed can also be mixed with an inert gas to aid in the atomisation process. After being injected, the feed contacts with the hot catalyst particles, that come from the regenerator, at the bottom of the riser vaporising almost instantly. The vaporised feed reacts on the surface of the catalyst particles, expanding in volume and propelling the (cracked) hydrocarbon vapours and the catalyst particles upward. Alongside the cracking reactions, where large hydrocarbon molecules are cracked into smaller ones, coke is also formed that deposits in the catalyst particles, deactivating them.

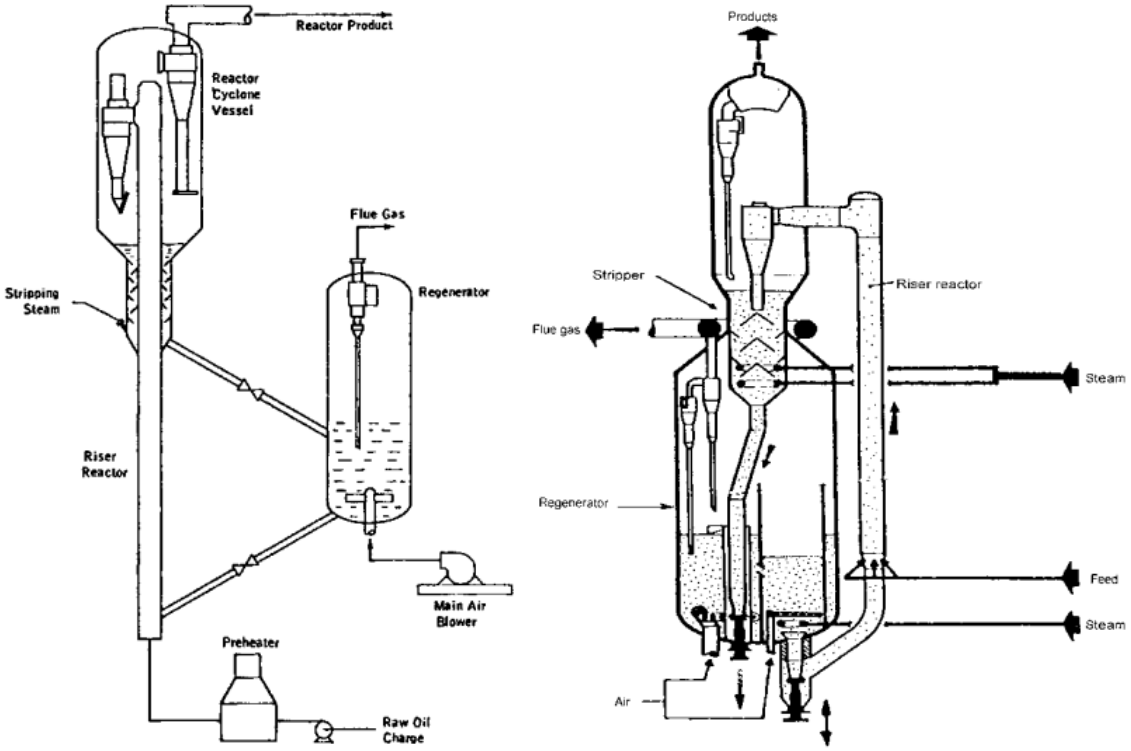

Figure 2.2 – Examples of the two possible FCCU configurations. Left: side-by-side. Right: stacked. Both retrieved from [8]

The riser terminates in a disengager, where a cyclone system, usually with two stages, separates the hydrocarbon vapours from the catalyst particles. The hydrocarbon vapours are sent to a downstream fractionation stage, while the catalyst particles drop to a stripper, where water vapour is injected to dislodge and recover any hydrocarbons mixed with the catalyst particles. Most of the hydrocarbons adsorbed on the catalyst particles are not recovered and constitute what is known as soft coke.

From the stripper the catalyst particles are sent to the regenerator. In the regenerator air is injected to burn off the coke present in the catalyst particles, regenerating their catalytic activity. After being regenerated, the catalyst particles are sent to the riser to once again participate in the cracking reactions. [3]

2.2.1 Riser

The main part of the reaction takes place in the riser, and, ideally, should be limited to the riser alone. Here the catalyst is transported by the lift media (before contacting the feed) and then mainly by the hydrocarbon vapours, which are expanding due to the increasing number of moles. The only heat inlet for the riser is the hot catalyst that mixes with the feed which provides all the heat required for the vaporisation and the cracking reactions. The riser terminates inside the disengager. [3]

2.2.1.1 Chemistry

The reactions that occur inside the riser are very complex and difficult to define. The main group of reactions that occur are the cracking reactions, defined as the breaking of a C–C bond [8]. Table 2.1 resumes the main reactions that take place in the riser. The reactions that occur in the riser are globally endothermic, leading to a reduction of the temperature along the riser. It should be noted that natural petroleum has very little or no olefins; as such, the olefins that react in the riser originate from the cracking reactions themselves.

Table 2.1 – Summary of the cracking reactions taking place in the riser. [1]

Reactant	*Reaction*	*Products*
Paraffins	Cracking	Paraffins + Olefins
Olefins	Cracking	LPG Olefins
	Cyclization	Naphthenes
	Isomerization	Branched Olefins (H Transfer → Branched Paraffins)
	H Transfer	Paraffins
	Cyclization Condensation Dehydrogenation	Coke
Naphthenes	Cracking	Olefins
	Dehydrogenation	Cyclo-olefins (Dehydrogenation → Aromatics)
	Isomerization	Naphthenes with different rings
Aromatics	Side-chain cracking	Unsubstituted aromatics + Olefins
	Transalkylation	Different alkylaromatics
	Dehydrogenation Condensation	Polyaromatics (Alkylation/Dehydrogenation/Condensation → Coke)

2.2.1.2 Hydrodynamics

The hydrodynamics inside the riser are usually considered to be plug flow with dispersion both for the hydrocarbons and for the catalyst particles. The catalyst particles are transported by the vapours of the cracked hydrocarbons, but their velocity is smaller than that of the hydrocarbon vapours. This is usually referred to as the slip velocity. This slip velocity is higher than the terminal velocity for a single particle due to the formation of catalyst clusters, which behave like a big particle and, as such, have a higher terminal velocity.

The other way that the flow can be explained in the riser is the core-annulus model, where free catalyst particles are transported with the vapour in the core of the riser and the region near the wall (annulus) has almost no flow of hydrocarbons and a downflow of catalyst.

As the reaction progresses there's an increase in the number of moles in the vapour phase, which causes the vapour to expand. This expansion is the greatest impulse for the transport of the catalyst. [3]

2.2.1.3 Catalyst deactivation

One of the most important reactions that take place in the riser is the reaction of coke formation. Coke is the generic name given to the species that form and are deposited in the catalyst and which lead to its deactivation. Coke is usually considered to be composed of polyaromatic compounds with a high molecular weight and low H/C ratio. This type of coke, produced in these types of reactions is called catalytic coke. The other types of coke include Conradson Carbon Residue coke (CCR coke) which is present in the feed of the FCC and soft coke which are hydrocarbons that remained adsorbed on the catalyst when it's sent to the regenerator, among other types. [3]

Other mechanisms for coke deactivation are metals that come with the feed and deposit on the catalyst causing changes in the crystal structure of the catalyst, which decreases the activity of the zeolite. This type of deactivation is irreversible, unlike the deactivation caused by coke, which is reversible with the catalytic activity regenerated in the regenerator.

The existence of permanent deactivation requires that the catalyst that circulates inside the FCCU to be regularly purged, with a make-up of fresh catalyst being added periodically. This constant purge and make-up leads to a distribution of residence time of the catalyst particles inside the FCCU. This mixture of catalyst particles with varying residence times that circulates in the FCCU is called equilibrium catalyst. [3]

2.2.2 Stripper/disengager

The riser terminates in the disengager. The purpose of this equipment is to separate the hydrocarbons, that were cracked in the riser, from the catalyst particles, which are now deactivated and lost most of their catalytic activity. This separation is desired to be as fast as possible to prevent over cracking, which results in undesirable fractions being created, such as dry gas. The disengager includes a two stage cyclone to separate the catalyst particles from the hydrocarbons. The hydrocarbons are sent to a downstream fractioning process, while the catalyst particles drop to a stripper via the diplegs.

In the stripper, the spent catalyst accumulates and is contacted with stripping steam. The stripper may have baffles or packing to improve the catalyst/steam contact. The steam displaces the entrained hydrocarbons in the catalyst, sending them to the downstream fractioning processes, but most of the adsorbed hydrocarbons on the catalyst remain with the catalyst particle when these are sent to the regenerator. These remaining hydrocarbons in the catalyst may react further to give lighter fractions. [3]

2.2.3 Regenerator

In the regenerator the spent catalyst is burned with air or air+oxygen to burn the deposited coke on the catalyst and restore the catalyst activity.

The regenerator generally contains two phases: a dilute phase, also known as freeboard, and a dense phase. In the dense phase is where most of the combustion takes place and where most of the catalyst is. The catalyst here may circulate either co or counter current with the air.

The regenerator may operate in either partial or complete combustion. In partial combustion, there is a significant amount of CO in the flue gases. In this case there is a need for a CO boiler downstream the regenerator. In complete combustion, all of the CO has already been burned to CO2. Some units, for example the R2R [6], may function in the two operating conditions, where the first regenerator vessel operates in partial combustion, to avoid the higher temperatures of complete combustion, and the second regenerator vessel operates in complete combustion, to minimise the amount of coke that remains in the regenerated catalyst and to maximise its activity at the riser inlet.

In some units, especially those that crack residue (RFCC), an external heat exchanger may be required to maintain the heat integration of the entire FCCU. As a residue feed forms more coke than other feeds, some of the heat generated from the burning of the coke must be removed to keep the FCC in heat balance. Such an external heat exchanger produces steam that may be used elsewhere in the refinery. [6]

2.2.3.1 Chemistry

As previously mentioned, the regenerator may operate in either partial or full combustion. In either case, the main reactions that take place are as follows: [5]

$$C_{(s)} + \frac{1}{2}O_{2(g)} \rightarrow CO_{(g)} \quad \textbf{1.1}$$

$$C_{(s)} + O_{2(g)} \rightarrow CO_{2(g)} \quad \textbf{1.2}$$

$$CO_{(a)} + \frac{1}{2}O_{2(g)} \rightarrow CO_{2(g)} \quad \textbf{1.3}$$

$$CO_{(g)} + \frac{1}{2}O_{2(g)} \rightarrow CO_{2(g)} \quad \textbf{1.4}$$

$$2H_{(s)} + \frac{1}{2}O_{2(g)} \rightarrow H_2O_{(g)} \quad \textbf{1.5}$$

Most of these reactions occur only in the dense phase, but those that take place only in the gas phase also occur in the freeboard. For this reason there is an increase in the temperature of the flue gases from when they leave the dense phase until they exit the regenerator, as most of these reactions are exothermic (afterburning).

In the regenerator, coke is burned off, which restores activity to the catalyst, but the high temperatures and the presence of steam also permanently deactivate the catalyst. This is what inspired the creation of the R2R regenerator design. The combustion of hydrogen, which forms steam has faster kinetics than the combustion of carbon. As such, most of the steam that would be formed from the combustion of coke is removed in the first regenerator vessel. Operating in partial combustion, it has a lower temperature, avoiding the dangerous combination of high temperatures and high steam concentration, which would permanently deactivate the catalyst faster. In the second regenerator, as most of the steam has already been formed and removed from the reacting environment, the operation can be in full combustion, to completely remove the remaining coke still on the catalyst.

Besides the combustion of carbon and hydrogen, there is also the combustion of sulphur and nitrogen. The combustion of these two elements form SO_x and NO_x, which are pollutants and whose emissions must be minimised. The addition of SO_x and NO_x reducers to the catalyst causes SO_3 to be reduced to H_2S and NO_x to be reduced to N_2 and NH_3.

The presence of combustion promoters catalyses the oxidation of CO to CO_2. This may not be desirable in a regenerator designed to operate in partial combustion, since there would be competition for the limited supply of oxygen: combustion of C to CO (to restore activity) and combustion of CO to CO_2.

2.2.3.2 Hydrodynamics

Inside the regenerator there are two different regions: the dense bed and the freeboard.

It's in the dense bed that most of the combustion to regenerate the catalytic activity takes place. Air, or an air and oxygen mixture, is injected at the bottom of the dense bed, fluidising the catalyst particles and burning off deposited coke.

In the freeboard, the catalyst particles are ejected from the surface of the dense phase and transported by the combustion gases. Most particles fall back down to the dense bed, but others are pneumatically transported. At the height where no more particles will return to the dense bed on their own there is a cyclone system the separate the remaining catalyst particles.

2.3 FCC Modelling

2.3.1 Riser

Modelling the riser is a very complex task due to the very complex hydrodynamics and an enormous amount of reactions that take place in it, between thousands of compounds that are impossible to individualise. As such, several assumptions and approximations must be made in order to create a model for the riser reactor present in the FCC.

The different parts that need to be modelled in a riser are:

- Feed atomisation and vaporisation
- Hydrodynamics

- Cracking kinetics
- Catalyst deactivation

2.3.1.1 Feed vaporisation

Most models model the feed vaporisation as instantaneous upon contact of the feed with the hot regenerated catalyst. This approximation is justified by the fact that with small enough droplets, the feed is completely vaporised in less than 5% of the total residence time, which in typical risers would correspond to a height of about 1.5 to 3 m. [9] Published models that model the feed vaporisation as following the above assumption include the model by Fernandes [3], Kumar et al. [10], Dasila et al. [11], and Ali and Rohani [12], among many others.

With this said, some models do account for the time and riser length in which feed vaporisation takes place. Examples include the model by Gupta [13] and others. [14]–[16]

In these models, the model must always consider three phases in the riser: the vapour phase (with the vaporised hydrocarbons and transport/atomisation steam), the solid phase (with the catalyst/catalyst clusters) and the liquid phase (feed droplets). The model must also consider the heat and mass transfer between these several phases, which is also dependent on the droplet size distribution.

When the model includes feed vaporisation that is not instantaneous, it may or may not include reactions during the time that the vaporisation takes place.

2.3.1.2 Hydrodynamics

The complex hydrodynamics inside the riser are hard to model. The most accurate way to model the hydrodynamics would be with a model based on Computational Fluid Dynamics (CFD). However, even though several such models have been constructed, they are only useful for modelling the hydrodynamics alone. A complete model of the riser, which would presumably be used, for example, for optimisation, should be simple enough that it can be calculated in a short amount of time, which a CFD based model is not capable of. [17]–[21]

In the other end of the spectrum lies the riser models that model the flow of the vapour phase and catalyst phase as plug flow. These types of model may or not include axial and radial dispersion. There is also the slip factor. The slip factor is simply defined as the ratio between the velocity of the vapour phase and the velocity of the catalyst phase. Some approximate this factor to 1 while others define it to be equal to the terminal velocity of the catalyst particles in the vapour phase, or the terminal velocity of the catalyst clusters in the vapour phase, in order to obtain slip factors close to those measured in real units. [22]

During the reaction there’s an increase in the amount of molecules in the vapour phase due to the cracking reactions, which causes the expansion of the vapour phase that ultimately is responsible for the acceleration of the solid phase throughout the riser. [3]

2.3.1.3 Cracking kinetics

The sheer number of components that both the feed and the products are made from makes it impossible to create a detailed kinetic model for every reaction that takes place in the riser. Such a model would require thousands and thousands of kinetic parameters, which in itself would be almost impossible to obtain, but would also require a detailed description of the FCC feed and products, which is almost never available in a refinery and could also be changing by the hour.

For all these reasons, the kinetic models used when modelling a riser usually lump the components. One of the most used kinetic models is the three lump model with the feed, gasoline and gas+coke as lumps. The need to calculate the amount of coke formed separately rapidly created a four lump model, where the gas and coke are calculated separately. Other lumped models have also been created, with up to 19 lumps or more being used. In these models, the reactions are considered to be lumps being cracked to form some amount of other lump or lumps. [10], [11], [23]–[28]

Another approach is to use the carbon number and/or the type of hydrocarbon and the reactions between these. This has the advantage of taking into account reactions that may not necessarily fall into other lumps (for example, a cracking reaction of a molecule in VGO may result in two other molecules also in VGO, or one that is in VGO and other in another lump). However, the kinetic parameters necessary for this type of model may be difficult to obtain or maybe the reaction cannot be generalized to a wide range of carbon number. [7], [29]–[31]

Another important reaction is the reaction of formation of coke. This reaction is very important because it's directly related with the deactivation of the catalyst. As such, every kinetic model must consider the formation of coke as one of the reactions and coke as one of the lumps. Because coke is such a difficult component to define, it also is one of the difficulties if one were to try and develop a detailed, molecule by molecule kinetic model.

2.3.1.4 Catalyst deactivation

The deactivation of the catalyst is usually modelled in one of two approaches: the time-on-stream and the coke-on-catalyst. [3]

The time on stream, as the name implies, uses a deactivation law that is dependent only on the time the catalyst spends in the riser. This has the advantage that it can encompass the several deactivation mechanisms that act upon the catalyst, besides only the deposited coke. However, it usually doesn't consider the coke on the catalyst inlet.

This is solved by using the coke on catalyst approach. In this approach, the catalyst activity is proportional to the mount of coke on the catalyst. This approach has the advantage of considering that the regeneration of the catalyst may not be total and that some coke may still be present on the catalyst at the riser catalyst inlet, and consequently not have all of its activity regenerated.

Whatever approach that is chosen, the deactivation is usually considered to affect all reactions equally. However this may not be necessarily true, as the deactivation of the catalyst may affect more one type of reaction than others, and as such the rate of consumption of a certain reactant or the rate of production of a certain product may not be affected in the same way as other reactions. The study by Corella [32] concluded that a model without selective deactivation is only slightly worse than one where the deactivation is selective to either the reactant or the products.

2.3.1.5 Thermodynamics

The temperature inside the riser varies with the length of the reactor because the reactions are endothermic. As such, the energy balance needs to be considered.

Models usually model the reactor as isothermal or adiabatic. The temperatures of the solids and of the vapours can be considered equal or there may be a temperature difference, which implies the use of heat transfer coefficients in the model. [13]

2.3.2 Regenerator

The regenerator is a fluidised bed reactor. Most fluidised bed models consider two regions: the dense region, where most of the solids are located and are in a fluidised state, and the dilute region, also called freeboard, where there are almost no solids.

The two regions of a fluidised bed model are modelled separately. The dense region is usually modelled with two interconnected phases: the fluidised solids and the gas. These two phases are given many different names by different authors for the different fluidisation regimes: for the solids phase there are “dense, emulsion, more dense, annulus, cluster, etc.” and for the gas phase “bubble, dilute, lean, void, core, less dense, etc.” The use of so many different names may induce some errors, as some names sometimes are used to distinguish between the dense region and the freeboard. To avoid such confusions this work adopts the nomenclature chosen by Abba [33] and Thompson et al. [34] for the dense region: low density (L) phase and high density (H) phase, which is valid for whatever fluidization regime is chosen.

2.3.2.1 Hydrodynamics

The freeboard is easier to model than the dense region, with some agreement between several authors that model this region as a 1D plug flow reactor, where the afterburning takes place (combustion of CO to CO2). [3]

The dense region is harder to model, as it has a more complex behaviour. One common way that it is modelled is with the two phase bubbling bed model. In this model there are two phases: the emulsion (H) and the bubbles (L). In the emulsion there are almost all of the solids and enough gas to maintain them in incipient fluidisation. The rest of the gas constitutes the bubble phase. Kunii and Levenspiel [35] have summarized all the common assumptions in their paper.

Some have also tried to model the dense region as a single phase. Although some authors claim results as good as the ones obtained for the two phase models, others claim that the results are not satisfactory. [7]

However, all of these models make the assumption that the bubbling bed model is a good approach to the regenerator hydrodynamics, not considering the other possible flow regimes. Following this same train of thought Abba [33], [36], [37] created a model that combines the bubbling bed, used in other models mentioned, with the turbulent fluidisation and fast fluidisation regimes through a probabilistic approach to which regime the flow actually resembles more, or even a combination of all three models.

2.3.2.2 Combustion kinetics

When modelling the combustion that takes place in the regenerator, different authors generally follow one of two approaches: either separate the combustion of carbon from the combustion of hydrogen, or assume that coke is composed of an anonymous hydrocarbon in the form of CH_x, where x is chosen by each author to be a certain value. In whatever approach, the combustion reactions don't usually distinguish different types of coke.

When modelling the combustion in a FCCU regenerator, often the combustion of H is either ignored or considered instantaneous. Faltsi-Saravelou et al. [5] have shown that this reaction should be explicitly considered, because of its significant thermal effects.

2.3.3 Stripper/disengager

Most models of the stripper and disengager don't separate them into different models, and are usually very simple models. Since almost no reactions take place in the stripper vessel, it is not very significant to a complete FCCU model.

The stripper is usually considered in dynamic models, where the catalyst residence time and hold up are significant for the dynamic response of the reactor. The striper may also be modelled to determine the amount of hydrocarbons that remained entrained with the spent catalyst when it is sent to the regenerator.

It is typically modelled as a continuous stirred tank (CST) where there is no reactions taking place. [3]

3 Model development

This chapter presents the work developed in modelling a regenerator of a FCCU and its evolution starting with the generalised fluidised bed reactor (GFBR) model from [33] and further simplifications. It also presents the modelling platform used.

3.1 Modelling platform

The regenerator model described in this chapter was developed in the modelling language gPROMS, using the software gPROMS ProcessBuilder 1.0.0. This modelling language and associated integrated modelling environments (including ProcessBuilder) were created and are maintained by Process Systems Enterprise.

gPROMS is a modelling language that allows the modelling of any equation based model. It possesses several capabilities that facilitate the writing of both algebraic and differential equations, which can include variables that can have as many domains as required, either discrete or continuous. The modelling environment also allows for connecting several models with simple and standardised connectors. This allows for the creation of libraries of different models that can be easily connected to construct a process in a flowsheet-like environment – e.g. connecting the outlet of a mixer to the inlet of a reactor and connecting the outlet of that same reactor to the inlet of a distillation column – without the need for any extra equations or "glue code". This process making ability is further augmented with the ability to customise the models in the flowsheet, allowing for a reduced number of models to create an endless number of processes that can be simulated.

Beyond modelling and simulating, ProcessBuilder also has tools for analysing experimental data, process optimisation, parameter estimation, among others. [38]

3.2 Generalised Fluidised Bed Reactor model

The regenerator model developed in this chapter was based on the generalised fluidised bed reactor model developed by Abba [33], [36], [37], itself an evolution of the model by Thompson et al. [34]. This model was used because it is the most complete fluidised bed reactor model found in literature.

This model differs from the traditional fluidised bed reactor models [35], [39]–[43] in that it doesn't assume *a priori* a specific flow regime. Instead, it consists of a generic reactor model (i.e. no flow regime assumptions) and a hydrodynamics properties model.

The reactor model itself is a fairly standard fluidised bed reactor model, where both the dense bed and the freeboard are modelled. The dense bed is also further divided into a low density phase and a high density phase. Each phase – dense bed-low density phase, dense bed-high density phase, and freeboard – is modelled as a dispersion reactor. The two phases of the dense bed communicate between each other through mass transfer. A diagram of the reactor model can be seen in Figure 3.1, retrieved from [33].

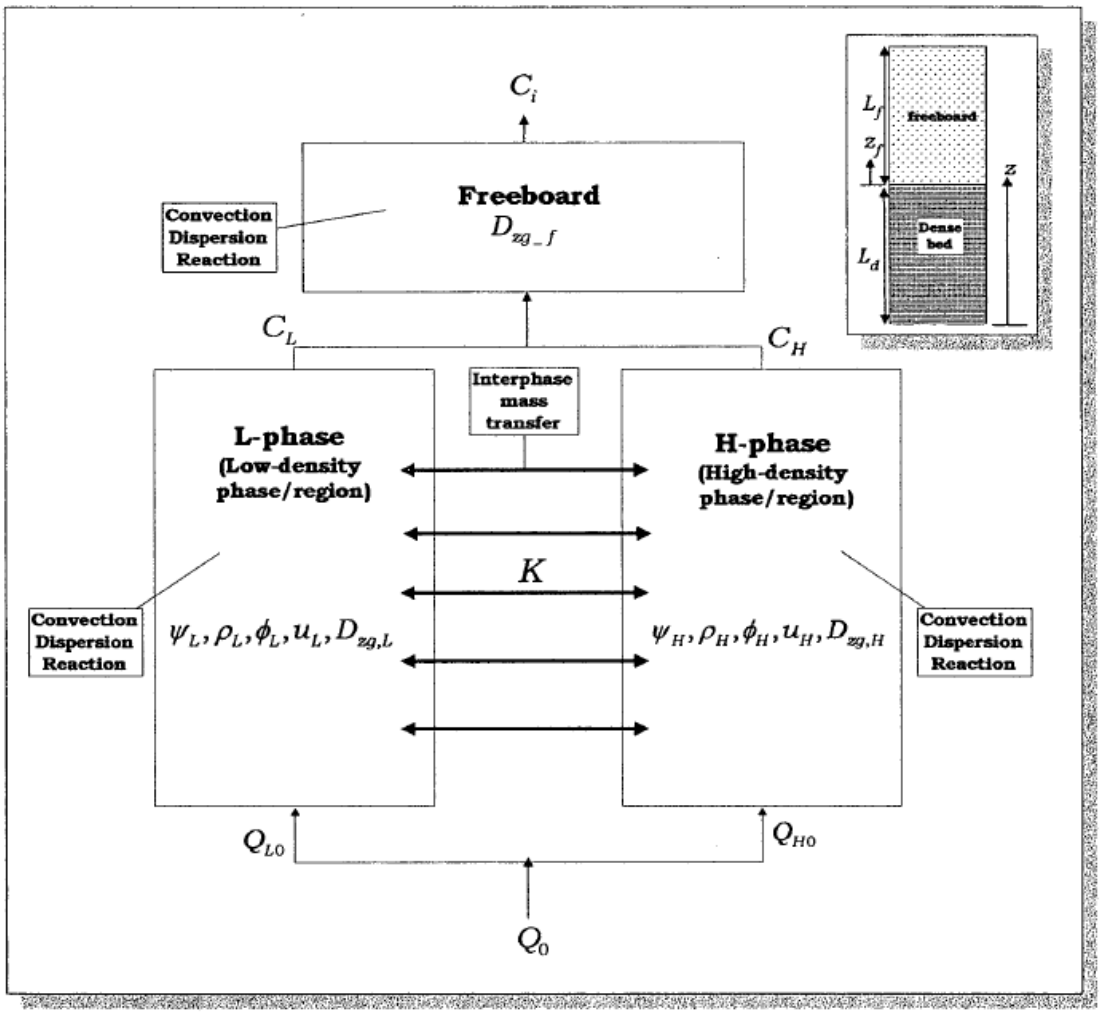

Figure 3.1 – Diagram of the reactor model in the GFBR model. [33]

In the properties model the flow regime calculations are performed for different flow regimes: in the case of this model for the bubbling, turbulent and fast fluidisation regimes. The part where this reactor model differs from traditional fluidised bed reactor model comes after the calculations for each different flow regime: while a traditional fluidised bed reactor model would then calculate in which flow regime the reactor is at the moment and use the corresponding values calculated for the determined flow regime, this model actually averages the value for each property based on the probability that the reactor is in each flow regime.

The differences of these two approaches can be easily seen in Figures 3.2 and 3.3, both retrieved from [33]. In the traditional approach the results of a single flow regime are used and, in the case that it calculates a regime transition, there is a sharp and sudden change in the value of the property calculated. In the probabilistic approach, the values of each property are averaged, using as averaging factors the probabilities of being in a certain flow regime, leading to a smooth change in the value of any given property calculated.

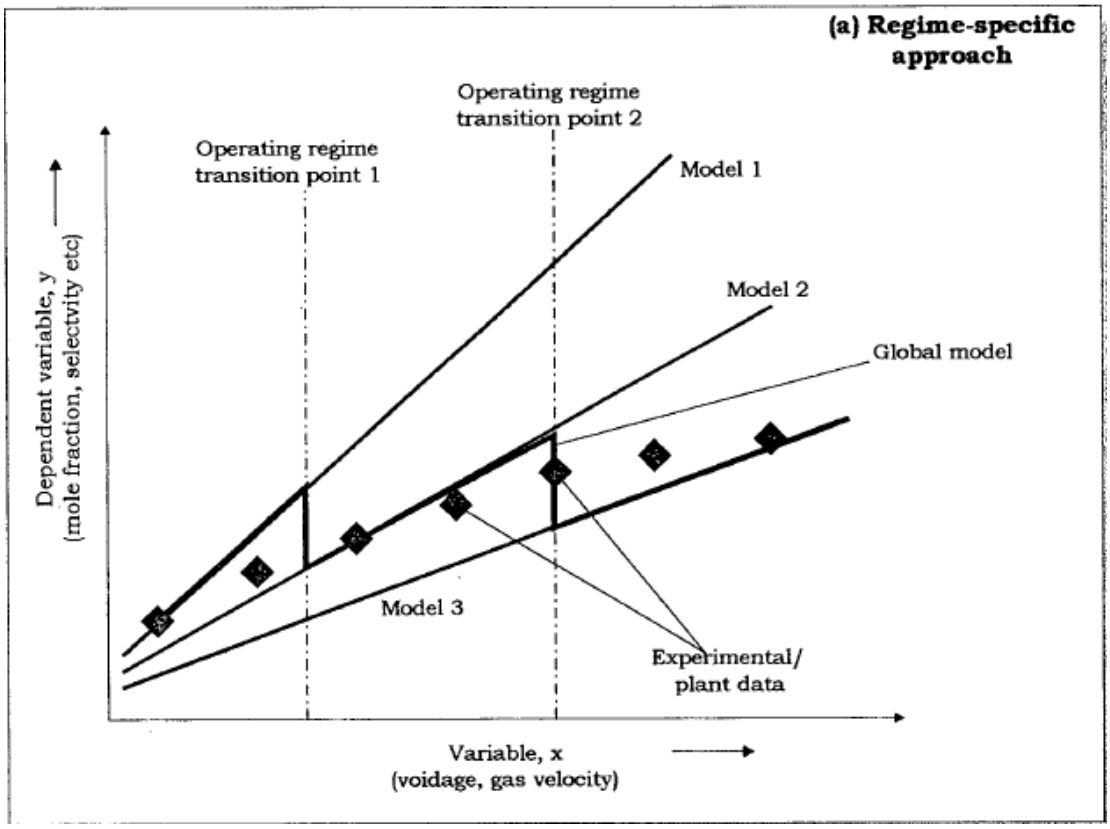

Figure 3.2 – Comparison of the value calculated for a variable x in the traditional fluidised bed reactor model approach with experimental data. [33]

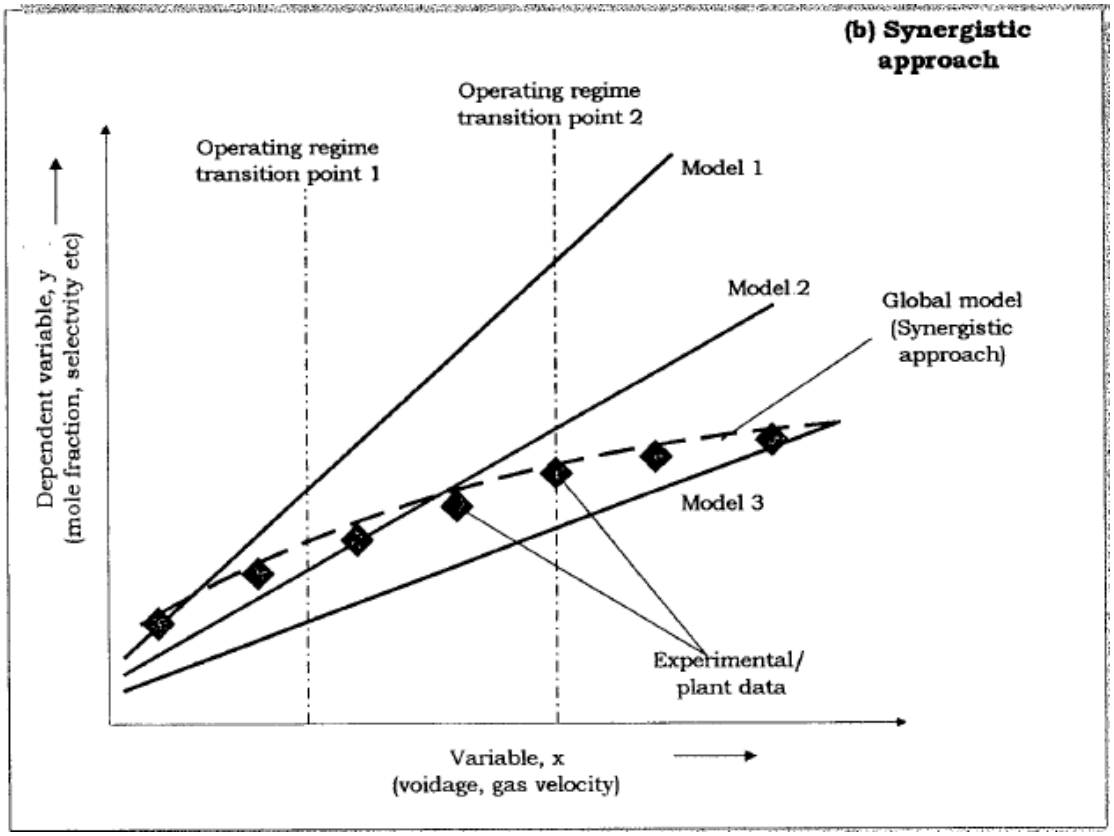

Figure 3.3 – Comparison of the value calculated for a variable x in the GFBR model approach with experimental data. [33]

3.3 GFBR model improvement

As the GFBR model was already implemented in gPROMS, the first step in implementing the regenerator model was to take the existing model and improve it so that it could be later adapted to create the regenerator model.

This improvement started by bringing the model up to date with the modelling standards of the latest gPROMS libraries. The model was initially developed to interface with the Process Model Libraries (PML), which have since been deprecated and replaced by the gPROMS Model Libraries (gML). This required some work as the different libraries act on different assumptions, e.g., the PML always assume reversible flow while the gML assume irreversible flow by default, and required the replacement of most variable types and connectors.

The next step in improving the existing GFBR model was to improve the modularity of the model. gPROMS includes facilities to easily connect models and use sub models inside higher level models, to improve model reusability and maintenance. Figure 3.4 represents a diagram of the original status of the GFBR model with its sub model structure represented. The original model lacks modularity, as can be easily seen in the figure, but also has a messy connectivity between the sub models and the higher level models, relying exclusively on equations on the highest level model, making the models cluttered and difficult to read and maintain. Instead, the connectivity should happen through connectors, which are objects in gPROMS that are well defined and allow for the connectivity of different models, as long as they use the same standard.

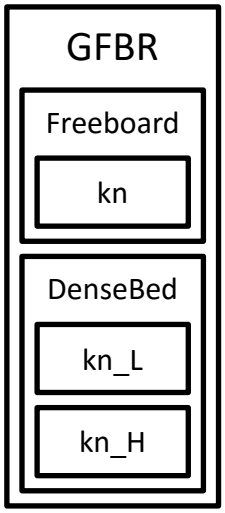

Figure 3.4 – Diagram of the initial structure of the GFBR model as implemented in gPROMS.

In the improved model, a diagram of which can be seen in Figure 3.5, it can be easily seen that the modularity has increased tremendously, even though the model is exactly the same as before. The connectivity was also improved, with the addition of the aforementioned connectors present in gPROMS. Unfortunately, it wasn't possible to replace all of the sub models connectivity with connectors due to time constraints.

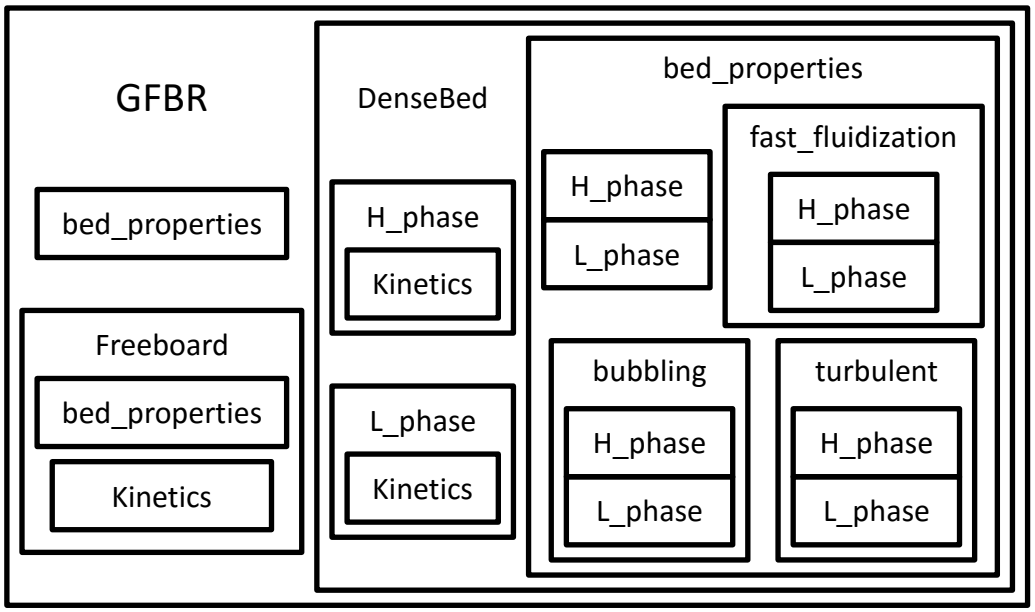

Figure 3.5 – Diagram of the final GFBR model structure as implemented in gPROMS.

The first important change in the model structure was separating the properties calculations from the reactor equations, creating separate models for calculating the hydrodynamic properties for each part of the reactor.

The second important change was separating the two phases of the dense bed, which ended up as being two instances of the same model, removing the need for repeated equations in the dense bed model itself.

The final important change to the model structure was separating the properties calculations in the dense bed into regime specific models, with the top level properties model responsible only for averaging the values calculated by each regime's model.

With the way it was done, the properties model of the dense bed is prepared to add, remove or replace any number of regime specific calculations with minimal work required. As long as the regime specific model complies with the same standard as the models already present in the properties model, it requires changing only a few lines of code, so that the properties model is aware of the new extra regime.

Besides the model restructuring, all of the equations and correlations used throughout the GFBR model were verified and corrected when necessary. Whenever possible, the correlations were also compared against their original source to guarantee that they were correct and valid.

3.4 Regenerator modelling

The main difference from a regenerator to a fluidised bed reactor is that in the regenerator there is net movement of the particles. While in a fluidised bed reactor generally there isn't net movement of the particles, with all of the particles remaining confined to the reactor, in the case of a regenerator of a fluid catalytic cracking unit, there is a constant entry of deactivated

catalyst, covered with coke, and a constant exit of regenerated catalyst, with the coke being burnt off inside the regenerator.

As such, there is the need to add an equation that handles the change in the coke content in the catalyst. The equation used assumes that the catalyst is perfectly mixed, that is, while the gas phase behaves like a dispersion reactor, the catalyst particles behave like a CSTR. Equation 3.1 shows how the interface between these two types of reactor model was implemented. It describes the mass balance of the elements present in the coke, typically considered to be carbon and hydrogen, but sometimes sulphur and nitrogen, among others, can also be considered. [5]

$$\frac{F_{c,in}Y_{k,in}}{MW_{ck}} = \frac{F_{c,out}Y_{k,out}}{MW_{ck}} - \int_0^{L_d} \Psi_L(z_d)\phi_L(z_d)\rho_p r_{cLk}(z_d)A_R dz_d - \int_0^{L_d} \Psi_H(z_d)\phi_H(z_d)\rho_p r_{cHk}(z_d)A_R dz_d - \int_0^{L_f} \phi(z_f)\rho_p r_{ck}(z_f)A_R dz_f \quad \textbf{3.1}$$

Due to the fact that the catalyst particles carry significant amounts of heat, the energy balance of the dense bed needed to be altered to reflect this. Equation 3.2 shows this, with the second term in the equation referring to this heat transport in the catalyst particles. The remaining two terms, the convective heat transfer by the gas phase and the dispersive heat transfer, respectively, remain unchanged from the original GFBR model. It should be noted that no heat transfer to the exterior environment or to a heat exchanger was considered, and the catalyst particles were assumed to be moving up, that is, the inlet of the catalyst is at the bottom of the regenerator. Equations 3.3 and 3.4 are the boundary conditions for the energy balance equation.

$$\frac{\partial}{\partial z_d}\left(h_g(z_d)\rho_g(z_d)U(z_d)\right) + \frac{\partial}{\partial z_d}\left(\frac{F_c}{A_R}C_{p_p}T(z_d)\right) - \frac{\partial}{\partial z_d}\left(k_e(z_d)\frac{\partial T(z_d)}{\partial z_d}\right) = 0 \quad \textbf{3.2}$$

$$-k_e(0)\left.\frac{\partial T}{\partial z}\right|_{z=0} = U(0)A_R\rho_g(0)C_{p_g}(0)\left(T_{in} - T(0)\right) + F_c C_{p_p}\left(T_{in} - T(0)\right) \quad \textbf{3.3}$$

$$\left.\frac{\partial T}{\partial z}\right|_{z=L} = 0 \quad \textbf{3.4}$$

For the gas phase, the mass balance was mostly unaltered, with only the reaction term being modified to consider the mass that the catalyst loses to the gas phase as it burns coke. Equations 3.5 and 3.6 represent the mass balances for the low density phase and the high density phase of the dense bed, respectively. Equations 3.7 and 3.8 represent the boundary conditions at the bottom of the reactor and Equations 3.9 and 3.10 at the top.

$$\frac{\partial}{\partial z_d}\left(\Psi_L(z_d)U_L(z_d)C_{Lk}(z_d)\right) - \frac{\partial}{\partial z_d}\left(\Psi_L(z_d)D_{zL}(z_d)\frac{\partial C_{Lk}(z_d)}{\partial z_d}\right) = \Psi_L(z_d)\phi_L(z_d)\rho_p r_{sLk}(z_d) + \Psi_L(z_d)\varepsilon_L(z_d)r_{gLk}(z_d) + k_{LH}a_I(z_d)\Psi_L(z_d)\left(C_{Lk}(z_d) - C_{Hk}(z_d)\right) \quad \textbf{3.5}$$

$$\frac{\partial}{\partial z_d}\left(\Psi_H(z_d)U_H(z_d)C_{Hk}(z_d)\right) - \frac{\partial}{\partial z_d}\left(\Psi_H(z_d)D_{zH}(z_d)\frac{\partial C_{Hk}(z_d)}{\partial z_d}\right)$$
$$= \Psi_H(z_d)\phi_H(z_d)\rho_p r_{sHk}(z_d) + \Psi_H(z_d)\varepsilon_H(z_d)r_{gHk}(z_d)$$
$$- k_{LH}a_I(z_d)\Psi_L(z_d)\left(C_{Lk}(z_d) - C_{Hk}(z_d)\right) \quad \textbf{3.6}$$

$$-D_{zL}(0)\frac{\partial C_{Lk}}{\partial z}\bigg|_{z=0} = U_L(0)\left(C_{Lk,in} - C_{Lk}(0)\right) \quad \textbf{3.7}$$

$$-D_{zH}(0)\frac{\partial C_{Hk}}{\partial z}\bigg|_{z=0} = U_H(0)\left(C_{Hk,in} - C_{Hk}(0)\right) \quad \textbf{3.8}$$

$$\frac{\partial C_{Lk}}{\partial z}\bigg|_{z=L} = 0 \quad \textbf{3.9}$$

$$\frac{\partial C_{Hk}}{\partial z}\bigg|_{z=L} = 0 \quad \textbf{3.10}$$

In the freeboard, the mass balance and the energy balance remained unchanged from the original GFBR model, except, again, for the addition of the reaction term relating to the burning of the coke. Equations 3.11 and 3.12 represent the mass balance and the energy balance of the freeboard, respectively.

$$\frac{\partial}{\partial z_f}\left(U(z_f)C_k(z_f)\right) - \frac{\partial}{\partial z_f}\left(D_z(z_f)\frac{\partial C_k(z_f)}{\partial z_f}\right) = \phi(z_f)\rho_p r_{sk}(z_f) + \varepsilon(z_f)r_{gk}(z_f) \quad \textbf{3.11}$$

$$\frac{\partial}{\partial z_f}\left(h_g(z_f)\rho_g(z_f)U(z_d)\right) - \frac{\partial}{\partial z_f}\left(k_e(z_f)\frac{\partial T(z_f)}{\partial z_f}\right) = 0 \quad \textbf{3.12}$$

For the hydrodynamic properties calculations, the exact same equations and correlations as the GFBR model were used. Refer to [33] for a detailed explanation of the correlations used and their reasoning.

As for the kinetic models, the models by Fernandes [3] and Faltsi-Saravelou et al. [5] were used. Although several other models for the combustion of coke exist in the literature [10], [11], [44]–[46], these two are the only ones that divide the reactions in carbon reactions and hydrogen reactions, instead of the combustion of a hydrocarbon in the form of CH_x, and present all of the required kinetic constants.

Both of these kinetic models have the same combustion reactions, presented in the chemical equations 1.1-1.5. The first two reactions are the combustion of the carbon present in the coke to carbon monoxide and carbon dioxide respectively. The next two reactions are the combustion of carbon monoxide. The difference between these two reactions is that in the first one the carbon monoxide is adsorbed on the surface of the catalyst particle and in the second the carbon monoxide is in the gas phase. Finally, the fifth reaction is the combustion of the hydrogen in the coke.

All other properties are calculated with the correlations found in [33] or with the ideal equation of state.

4 Simulation results

This chapter presents a case study to validate the regenerator model developed in the previous chapter, and compares it against some real plant data. The model was tuned to better adjust the model predictions to the data. Finally, a sensitivity analysis was performed on some key variables. Notably, the variables usually used as manipulated variables for controlling the regenerator were studied. The variables adjusted in the model tuning were also studied.

4.1 Case study

Faltsi-Saravelou et al. [5] presented this case study. In this paper, the authors use the model they developed in the first part of the paper [43], where they try to validate their fluidised bed reactor model. Data from this paper were used because it was the only one found that had the complete input data necessary for a regenerator model, with some minor omissions that were assumed.

This lack of test cases is due to the fact that most regenerator models found in literature are implemented as part of a complete FCCU, so only the input data necessary to simulate the entire unit is given, or not presented at all. Most notably, the data that is missing is the data that deals with the interface between the riser and the regenerator, as those values would be calculated by the model developed by each author.

Table 4.1 presents the input data used for the simulation. This will be referred to as the “base” simulation throughout this chapter. This data comes from the mentioned paper by Faltsi-Saravelou et al. [5]

Of the values used in the simulation, the only ones that weren’t found in the paper [5] were the air composition and the catalyst particles heat capacity. For these parameters the values presented in [3] were used.

4.2 Model validation

The results of the base simulation using the two kinetic models presented are compared against the data presented in [5] and the results of their own simulation in Table 4.2. Henceforth, the kinetic model from Fernandes [3] will be represented as K1 and the kinetic model from Faltsi-Saravelou et al. [5] will be represented as K2.

The model presented and used in [5] assumes that the regenerator works in the bubbling regime and represents the dense bed as a CSTR.

As can be seen in Table 4.2, the regenerator model developed in this work with both kinetic models gives good results in terms of the carbon conversion and temperatures inside the regenerator.

Table 4.1 – Input data for the base simulation of the regenerator model.

Parameter	*Value*
Reactor height (m)	19
Reactor diameter (m)	6.84
Catalyst particle diameter (μm)	86
Catalyst particle sphericity (-)	1
Catalyst particle density (kg m^{-3})	880
Catalyst particle heat capacity (J kg^{-1} K^{-1})	1200
Catalyst hold-up (kg)	51717
Air flowrate (kg s^{-1})	32.05
Air composition (%mol)	O_2: 20.7; N_2: 77.7; H_2O: 1.6
Air temperature (ºC)	183
Air pressure (atmg)	2.4
Catalyst flowrate (ton h^{-1})	885
Catalyst composition	$CH_{0.85}$
Catalyst carbon content (%$kg_C/kg_{catalyst}$)	0.87
Catalyst temperature (ºC)	512.7
Catalyst pressure (atmg)	2.4

Table 4.2 – Simulation results for both kinetic models and comparison with simulation results from Faltsi-Saravelou et al. [5] and real plant data.

	Measured data [5]	*Simulation results – [5]*	*Simulation results – K1*	*Simulation results – K2*
Bubbling regime probability	--	1	0.123	0.121
T dense bed (K)	1000	996	998.3	996.4
T freeboard (K)	1005	1008	1020.1	1003.7
Carbon on regenerated catalyst (%$kg_C/kg_{catalyst}$)	0.03	0.09	0.020	0.039
Carbon conversion (%)	96.6	89.7	97.7	95.5
Combustion gases (dry) (%mol)				
Oxygen	2.00	1.67	2.15	2.51
Carbon monoxide	0.03	0.03	0.0016	0.00006
Carbon dioxide	16.20	16.24	16.14	15.77
Void fraction (m^3 m^{-3})	--	0.80	0.66	0.66
Dense bed height (m)	--	8	4.4	4.4
L phase fraction (m^3 m^{-3})	--	--	0.362	0.360
Coke burnt in freeboard (%)	--	8.3	3.3	2.9

Comparing against the model developed in the article from which the plant data was retrieved [5], the model developed in this work gives much better results for the carbon conversion with both kinetic models used. However, the calculated values for temperature are slightly different from the plant data. The model developed in this work with the K2 gives the best results in this case, closely followed by the results from the article [5] itself. Lastly are the results with the kinetics K1. The composition of the combustion gases is also different from the expected values, with the calculated carbon monoxide content being much lower than expected with both kinetic models by orders of magnitude.

When comparing the values for which there are only simulation results and no real plant data, it can be easily verified that the hydrodynamic regime is very different between the article [5] and the results from this work. The first big difference is that the article assumes the bed is in the bubbling regime. However, the model from this work calculates that the bed has only a 12% probability of being in that flow regime. This is the biggest advantage of this model: it doesn't assume *a priori* a flow regime, but calculates an average of three flow regimes, that way being able to also mix different flow regimes and better approach reality. [33]

The remaining values that can be compared are the height of the dense bed and its void fraction and the amount of coke that is burnt in the freeboard and not in the dense bed. The height of the dense bed and the void fraction are very different, which is a result of the different approaches in the hydrodynamics models used. As for the coke burnt in the freeboard, the results from the article have more coke being burnt in the freeboard when compared with the two simulations in this work. This may be because of the fact that the article considers the dense bed to be a CSTR, and as such the extent of the combustion is lower.

4.2.1 Results analysis

In this section, the regenerator axial profiles generated with the model developed in this thesis will be analysed. Unfortunately there isn't enough data in literature with which to compare to, either results from other models or real data of axial profiles in regenerators.

The profiles that will be studied are those of the temperature, gas composition, superficial velocity, void fraction and the rates of combustion of both the carbon and the hydrogen in the coke.

On all of the plots, the two solid lines represent the base simulation for each of the kinetic models used, and the vertical dashed line represents the separation between the dense bed (0 to 4.4 m) and the freeboard (4.4 to 18 m).

Figure 4.1 presents the temperature axial profile results of the base simulation (as defined in Table 4.1) for both kinetic models tested. As can be seen in the figure, both kinetic models predict a similar temperature variation in the dense bed, with an average difference of approximately 2 K. In the freeboard, the kinetic model from Fernandes predicts a substantial increase in the temperature, creating a difference of about 18 K with the predictions of the other kinetics model.

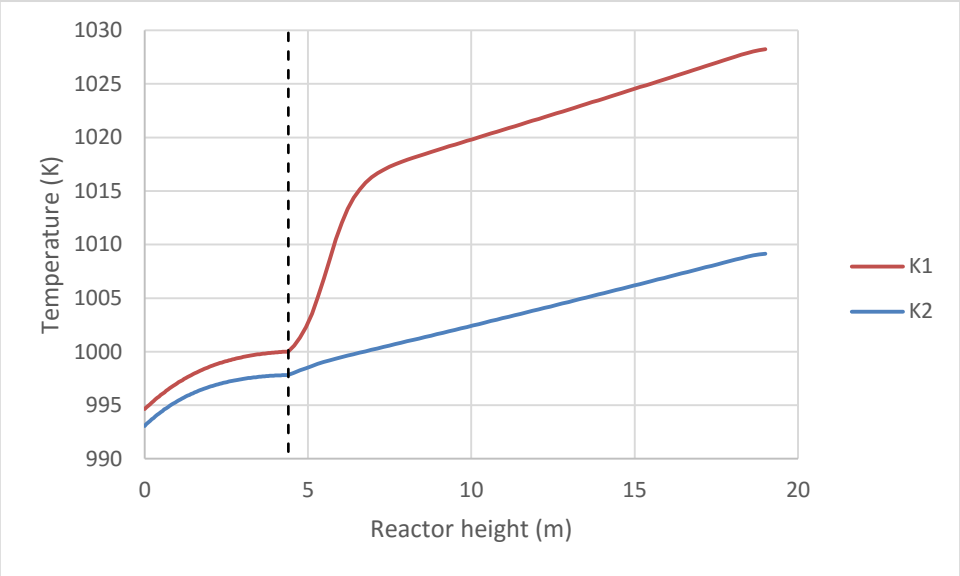

Figure 4.1 – Axial profile of the temperature in the regenerator for both kinetics models in the base simulation.

Figure 4.2 presents the oxygen molar fraction axial profile results of the base simulation (as defined in Table 4.1) for both kinetics models tested. The oxygen profiles predicted by both kinetics models are similar, with a rapid consumption of oxygen in the dense bed and very little consumption in the freeboard.

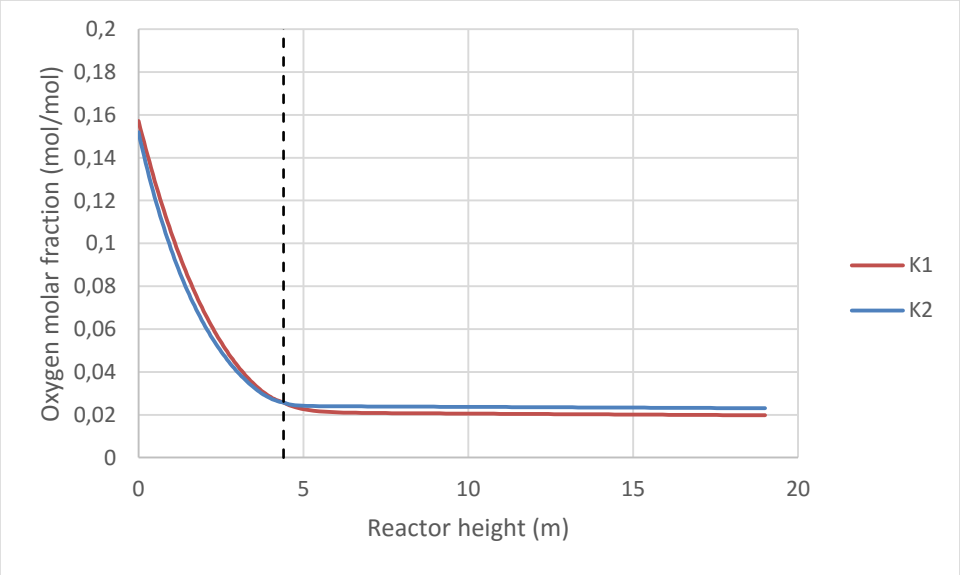

Figure 4.2 – Axial profile of the oxygen molar fraction of the gases inside the regenerator for both kinetics models in the base simulation.

Figure 4.3 presents the carbon dioxide molar fraction axial profile results of the base simulation (as defined in Table 4.1) for both kinetics models tested. The carbon dioxide profiles predicted by both kinetics models are similar, with a rapid generation of carbon dioxide in the dense bed and very little generation in the freeboard. This is the expected result, as most of the combustion occurs in the dense bed.

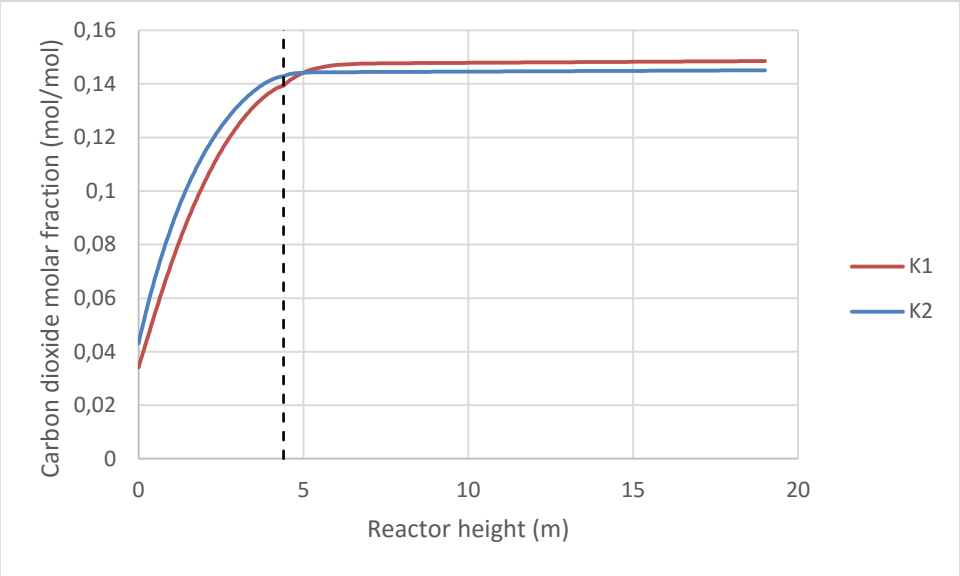

Figure 4.3 – Axial profile of the carbon dioxide molar fraction of the gases inside the regenerator for both kinetics models in the base simulation.

Figure 4.4 presents the carbon monoxide molar fraction axial profile results of the base simulation (as defined in Table 4.1) for both kinetics models tested. Here is where the biggest difference between the two kinetics models tested is observed. The kinetics model from Fernandes has a lower heterogeneous combustion rate of carbon monoxide, which leads to a higher concentration of carbon monoxide in the dense bed. In the freeboard, the homogenous combustion is dominant, leading to a rapid decrease in the carbon monoxide concentration to the same levels as the other kinetics model. The kinetics model of Faltsi-Saravelou et al. results in lower concentrations of carbon monoxide in all of the reactor.

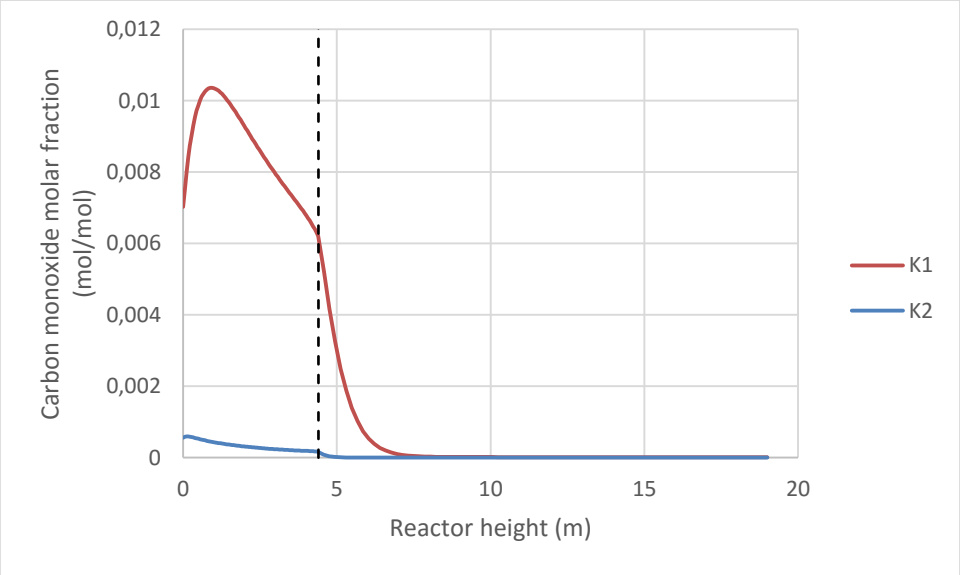

Figure 4.4 – Axial profile of the carbon monoxide molar fraction of the gases inside the regenerator for both kinetics models in the base simulation.

Figure 4.5 presents the water molar fraction axial profile results of the base simulation (as defined in Table 4.1) for both kinetics models tested. The water concentration profile is almost the same for both of the kinetics models used, with a steady increase of the concentration in the dense bed, stabilising in the freeboard.

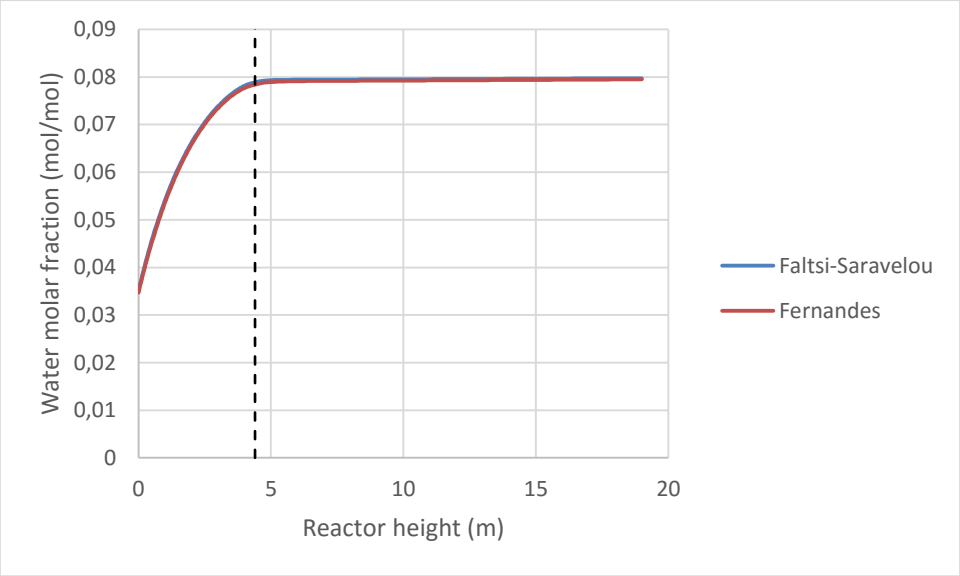

Figure 4.5 – Axial profile of the water molar fraction of the gases inside the regenerator for both kinetics models in the base simulation.

Figure 4.6 presents the superficial velocity axial profile results of the base simulation (as defined in Table 4.1) for both kinetic models tested. It can be easily seen that the superficial velocity follows the temperature profile (Figure 4.1) for both kinetic models tested. The only noteworthy observation is the jump in the superficial velocity at the interface of the dense bed and freeboard.

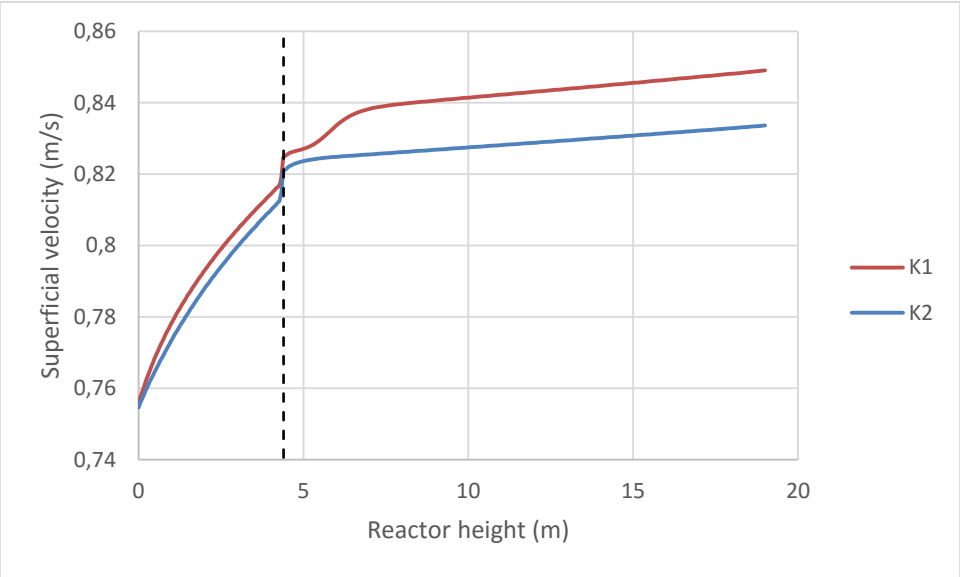

Figure 4.6 – Axial profile of the superficial velocity of the gases inside the regenerator for both kinetics models in the base simulation.

Figure 4.7 presents the void fraction axial profile results of the base simulation (as defined in Table 4.1) for both kinetics models tested. There is almost no difference in the results of the void fraction profile using either of the kinetics models. This is to be expected as the hydrodynamics model is not affected by the kinetics. It can be easily seen that the void fraction is almost constant in the dense bed and increases exponentially in the freeboard as expected.

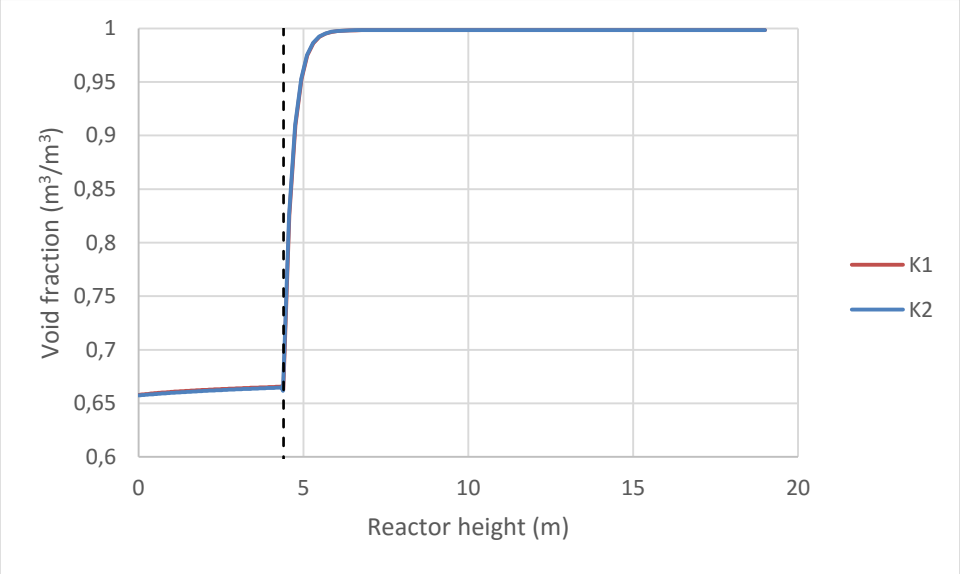

Figure 4.7 – Axial profile of the void fraction of the solids inside the regenerator for both kinetics models in the base simulation.

Figure 4.8 presents the carbon combustion rate axial profile results of the base simulation (as defined in Table 4.1) for both kinetics models tested. Both kinetics models have similar profiles for the carbon combustion rates, but with different values. This is to be expected because in both models this rate depends heavily on the oxygen concentration, with the profiles following the curve of the oxygen concentration profiles (Figure 4.2), with the difference in values due to their different kinetic constants.

Figure 4.9 presents the hydrogen combustion rate axial profile results of the base simulation (as defined in Table 4.1) for both kinetics models tested. Like the carbon combustion rate, both kinetic models have different hydrogen combustion rates, but their profile is similar, following the oxygen concentration profile (Figure 4.2).

4.2.2 Model tuning

As said before, the results of the developed model regarding temperature and combustion gases composition are different from the expected values. For this reason, an attempt was made to try to match those results by changing some parameters in the simulation.

The first parameter used was the catalyst particles heat capacity. It was decided to use this parameter because the heat capacity, which greatly influences the reactor temperature, used in the simulation came from a different source from the rest of the parameters.

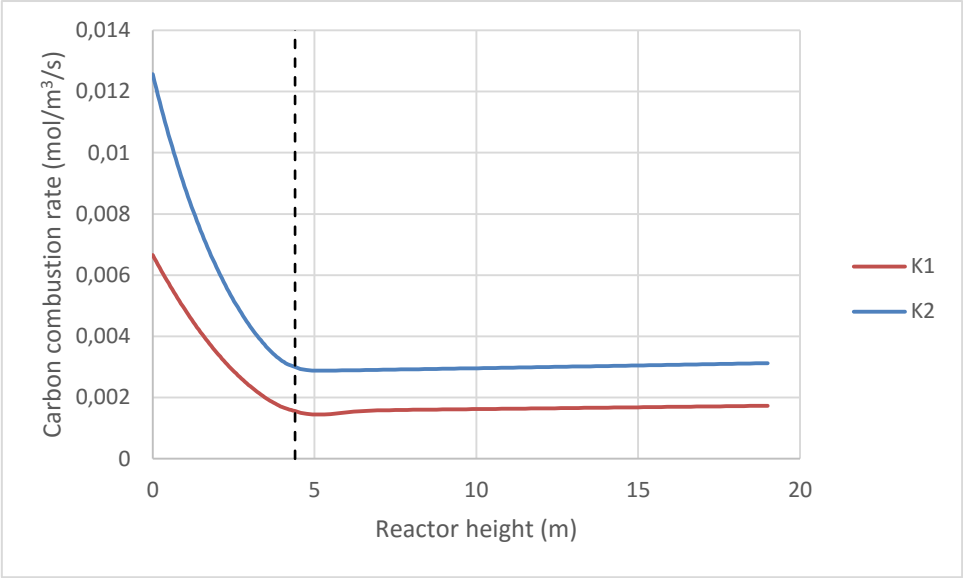

Figure 4.8 – Axial profile of the rate of the combustion of the carbon in the coke for both kinetics models in the base simulation.

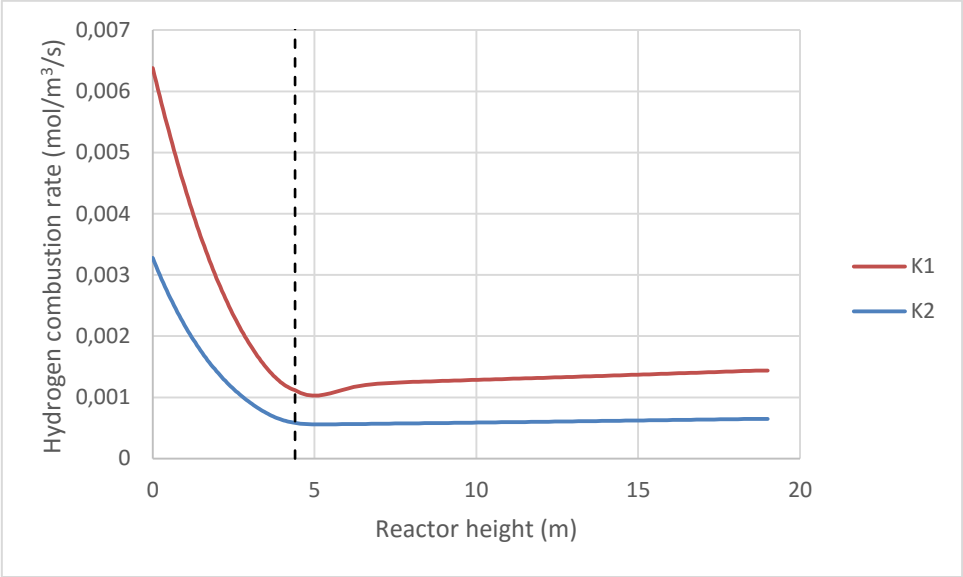

Figure 4.9 – Axial profile of the rate of the combustion of the hydrogen in the coke for both kinetics models in the base simulation.

The other parameters that were tuned were three new parameters introduced in the kinetic model to adjust the rates of the combustion of carbon, the combustion of hydrogen and the combustion of carbon monoxide (both heterogeneous and homogeneous). These parameters should affect both the temperature (due to the heat of reaction) and the composition of the outlet gases.

To perform this fitting of the parameters, the Parameter Estimation tool of gPROMS ProcessBuilder was used. The objective values used to perform the estimation were the temperatures in the dense bed and freeboard, and the outlet carbon content of the catalyst.

The new values of the parameters are presented in table 4.3, with the comparison of the results being presented in table 4.4.

Table 4.3 – Summary of the values fitted in the parameter estimation: base values and values fitted for both kinetic models.

	Particle heat capacity [J kg^{-1} K^{-1}]	*Combustion rate – Carbon [-]*	*Combustion rate – Hydrogen [-]*	*Combustion rate – Carbon monoxide [-]*
Base values	1200	1	1	1
Tuned values – K1	1197.2	0.68	1	93
Tuned values – K2	1200	1.33	1	1

Table 4.4 – Simulation results with the fitted values in the parameter estimation and comparison with the results of the simulations with the unfitted values and the measured data.

	Measured data	*Base simulation – K1*	*Base simulation – K2*	*Tuned simulation – K1*	*Tuned simulation – K2*
Bubbling regime probability	--	0.123	0.121	0.121	0.121
T dense bed (K)	1000	998.3	996.4	**998.5**	**998.7**
T freeboard (K)	1005	1020.1	1003.7	**1006.5**	**1005.8**
Carbon on regenerated catalyst (%kg$_C$/kg$_{catalyst}$)	0.03	0.020	0.039	**0.030**	**0.030**
Carbon conversion (%)	96.6	97.7	95.5	96.6	96.6
Combustion gases (dry) (%mol)					
Oxygen	2.00	2.15	2.51	2.34	2.33
Carbon monoxide	0.03	0.0016	0.00006	0.00002	0.00006
Carbon dioxide	16.20	16.14	15.77	15.94	15.95
Void fraction (m^3 m^{-3})	--	0.66	0.66	0.66	0.66
Dense bed height (m)	--	4.4	4.4	4.4	4.4
L phase fraction (m^3 m^{-3})	--	0.362	0.360	0.360	0.360
Coke burnt in freeboard (%)	--	3.3	2.9	3.2	2.8

Something that is worth mentioning is that changing the rate of combustion of hydrogen resulted in almost no difference in the final results. This effect will be studied in more detail in the sensitivity analysis. The same can also be said about the rate of combustion of carbon monoxide, evidenced by the fact that for one of the kinetics models the rate remained unchanged and for the other the new rate is 93 times the original one for the results to be noticeable.

4.3 Model simplifications

In most models presented in the literature, the model of the regenerator is simplified in some way. Specifically, the hydrodynamic model chosen for the dense bed and for the freeboard is simpler than the ones used in this thesis.

In this thesis, the dense bed model considers two phases, which are interconnected and each phase is modelled as a dispersion reactor. Simpler models may choose to represent one or the two phases as a CSTR or as a plug flow reactor. Some models even lose the distinction between the two phases and choose to model the dense bed as a single pseudo-phase, usually modelled as a plug flow reactor or as a CSTR.

Some work has been done to try to understand the difference of the results given by each model. Vale (cited in [3]) tested four different models and concluded that the model that best represented the regenerator was a single phase CSTR. A possible conclusion from this result may be that the dispersion is an important factor when modelling a regenerator, since a plug flow reactor would be a more intuitive representation for this type of reactor, when compared with a CSTR.

As such, an effort was made to simplify the base model presented in this thesis (cf. Chapter 3) and compare all common models of regenerator commonly found in literature. Table 4.5 represents the different options used to model each part of the regenerator, represented graphically in figure 4.10. Table 4.6 presents the results of the simulation using those models.

Table 4.5 – Summary of the different reactor models used to model each part of the regenerator in each simplified model.

		M0	*M1*	*M2*	*M3*	*M4*
Freeboard		Dispersion	PFR	PFR	PFR	PFR
Dense bed	L-phase	Dispersion	PFR	PFR	CSTR	CSTR
	H-phase	Dispersion	PFR	CSTR	CSTR	

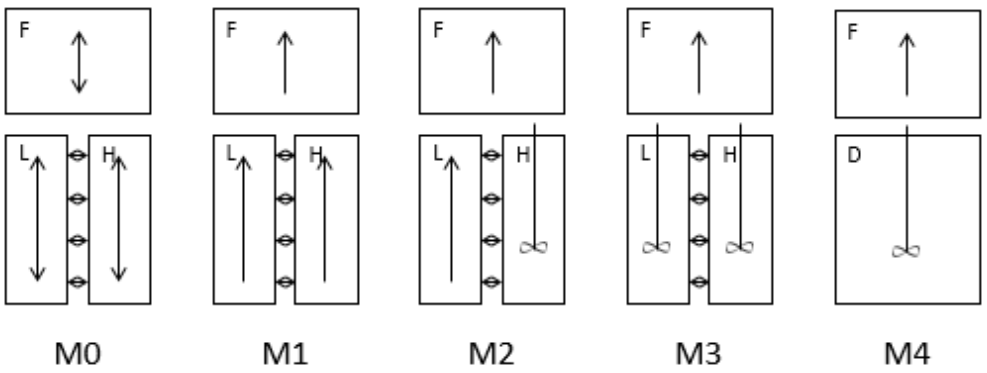

Figure 4.10 – Representation of the different model simplifications compared with the base model.

Table 4.6 – Main simulation results for the different simplified models and comparison with the base model and measured data.

	Measured data [5]	*M0*	*M1*	*M2*	*M3*	*M4*
T dense bed (K)	1000	998.3	998.4	1182.8	1206.5	1205.5
T freeboard (K)	1005	1020.1	1004.2	1191.1	1223.3	1226.2
Carbon on regenerated catalyst (%$kg_C/kg_{catalyst}$)	0.03	0.020	0.031	0.018	0.006	0.008
Carbon conversion (%)	96.6	97.7	96.4	97.9	99.3	99.1
Combustion gases (dry) (%mol)						
Oxygen	2.00	2.15	2.41	0.60	2.71	2.09
Carbon monoxide	0.03	0.0016	0.00005	0.00002	0.00002	0.00002
Carbon dioxide	16.20	16.14	15.87	17.44	15.67	16.18
Coke burnt in freeboard (%)	--	3.3	2.20	4.57	7.53	7.84

The nomenclature of the simplified models in the tables and figure is as follows:

- M0 – base model, without any simplification
- M1 – base model without any dispersion
- M2 – model M1, but with the high density phase of the dense bed replaced with a CSTR
- M3 – model M2, but with the low density phase of the dense bed also replaced with a CSTR
- M4 – model M1 with the dense bed replaced with a single CSTR

One important note must be made that the implementation of the model simplifications were not handled correctly, as evidence by the following:

- For model M2, where the high density phase of the dense bed is modelled as a CSTR and the low density phase as a PFR, there are problems with the mass balance. Even though the amount of oxygen in the combustion gases is much lower compared with the results of model M0, the carbon conversion is approximately the same.
- For the models involving a CSTR – models M2, M3 and M4 – there are problems with the energy balance. The average temperature in both the freeboard and dense bed is approximately 200 K above those obtained with the more complex model (model M0) and the measured data.

Comparing the base model M0 with the model where every phase is replaced with a PFR (model M1), we see that the results obtained are better than those obtained with the more complex model presented in this thesis, closer to those obtained when the model was tuned with the kinetic model of Faltsi-Saravelou et al. [5]

Figure 4.11 compares the axial profiles of the carbon dioxide molar fraction for the models M0 and M1. Models M2 to M4 are not included in this comparison for the reasons stated before. The carbon dioxide concentration is used as an example to compare the difference in these two models. As such, no other variables will be compared.

In this figure, it can be concluded that, although the outlet values of the carbon dioxide concentration are similar, the profiles inside the reactor are not. This is especially true in the dense bed region, where most of the combustion takes place.

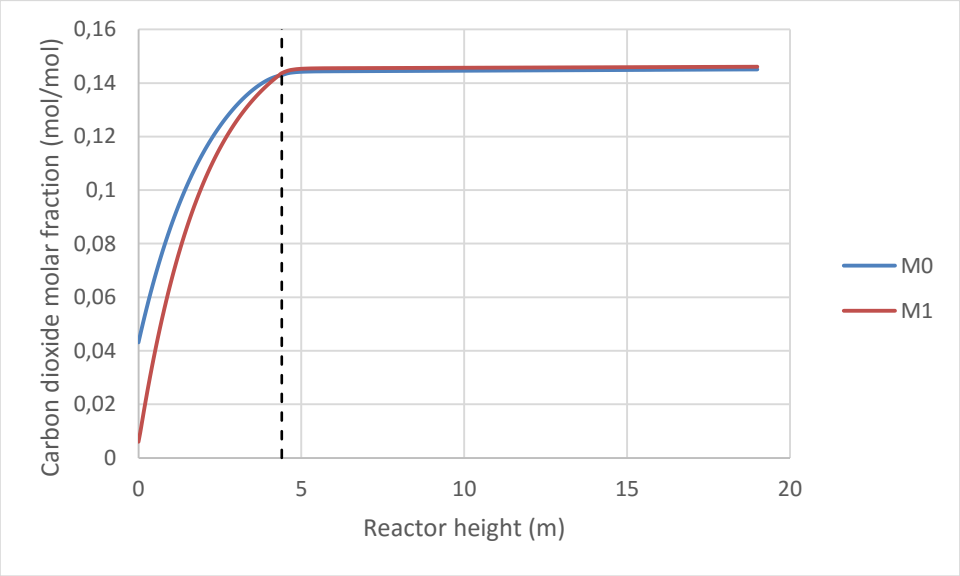

Figure 4.11 – Comparison of the axial profiles of the carbon dioxide molar fraction for the models M0 and M1.

4.4 Sensitivity analysis

In this section the sensitivity analysis was performed only with the kinetic model from [5]. The variables studied were:

- Catalyst particle heat capacity
- Carbon combustion rate
- Hydrogen combustion rate
- Carbon monoxide combustion rate
- Air flowrate
- Catalyst flowrate
- Catalyst temperature
- Catalyst coke content

The first four variables studied in this analysis are those obtained in the model tuning (section 4.2.2.). The next two variables are those usually used as manipulated in controlling the regenerator. The final two variables cannot be directly manipulated, but influence the operation of the regenerator, which is why they were included.

On all of the following plots, the base simulation value is marked by a vertical dashed line.

4.4.1 Particle heat capacity

It is easily verified that the relationship between the heat capacity of the catalyst particles and the temperature inside the regenerator is almost linear: the higher the heat capacity, the lower the temperature inside the regenerator, since the catalyst particles act as a heat sink for the energy released in the combustion of the coke. (Figure 4.12)

The decreasing temperature decreases the combustion reaction rates, which in turn affect the content of the combustion gases and the amount of carbon still present in the catalyst particles at the regenerator outlet: less coke being burnt results in more carbon left over in the catalyst particles, more oxygen in the combustion gases and less carbon dioxide. (Figures 4.13 and 4.14)

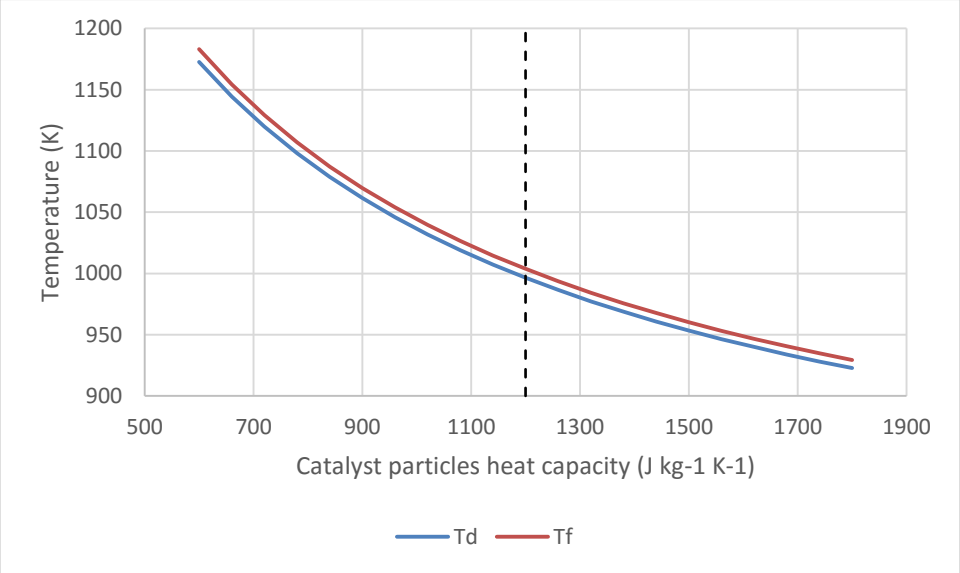

Figure 4.12 – Variation of the average temperature in the dense bed and freeboard with the catalyst particles heat capacity.

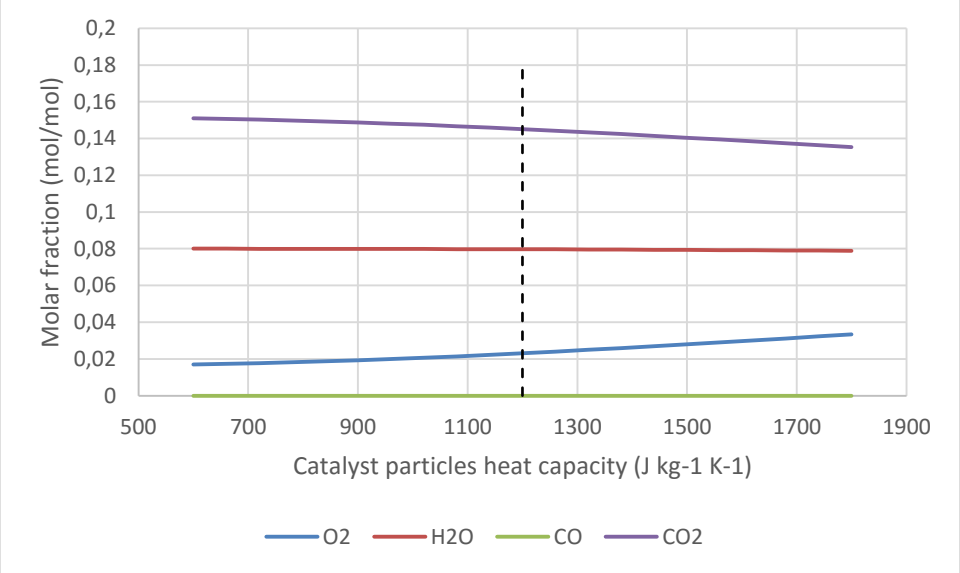

Figure 4.13 – Variation of the outlet gas composition with the catalyst particles heat capacity.

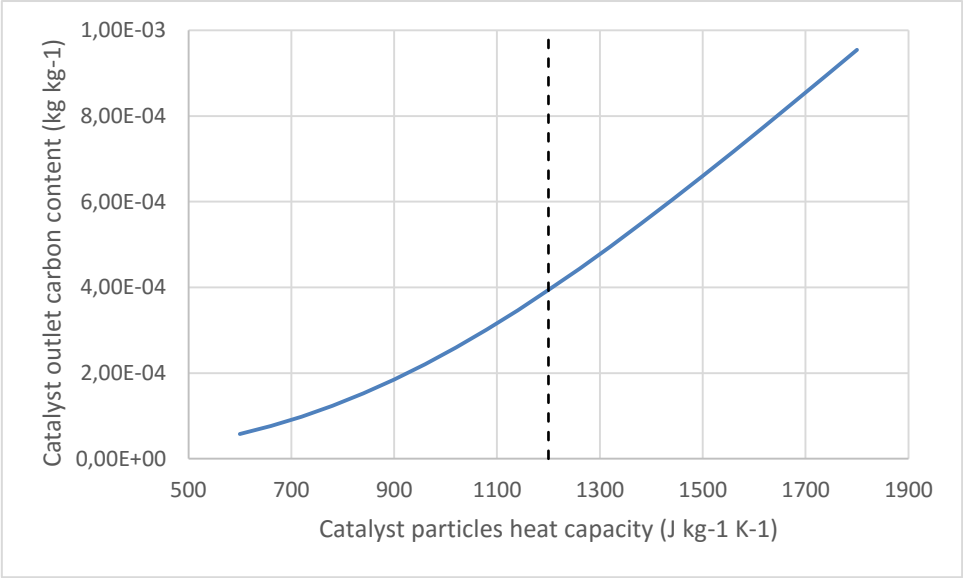

Figure 4.14 – Variation of the carbon content of the catalyst particles at the outlet with the catalyst particles heat capacity.

4.4.2 Carbon combustion rate

The results of this sensitivity analysis are those that intuitively would be expected. Increasing the combustion rate of carbon decreases the carbon in the catalyst particles at the regenerator outlet (Figure 4.17). With more carbon being burnt, more energy is released and the temperature inside the regenerator increases (Figure 4.15). The amount of carbon dioxide also increases, while the amount of oxygen decreases. The amount of water in the combustion gases increases only slightly, as it is affected only by the combustion of hydrogen (Figure 4.16).

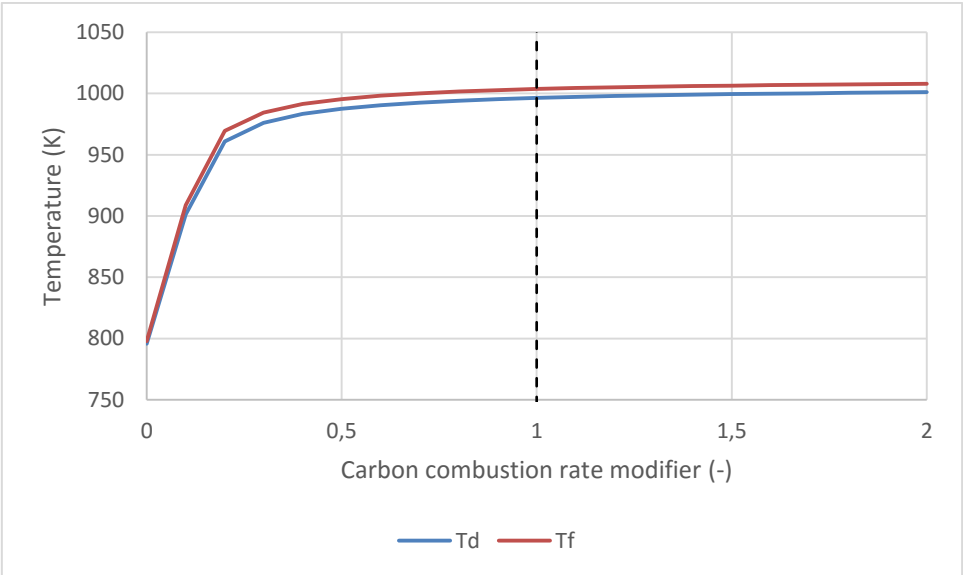

Figure 4.15 – Variation of the average temperature in the dense bed and freeboard with the carbon combustion rate modifier.

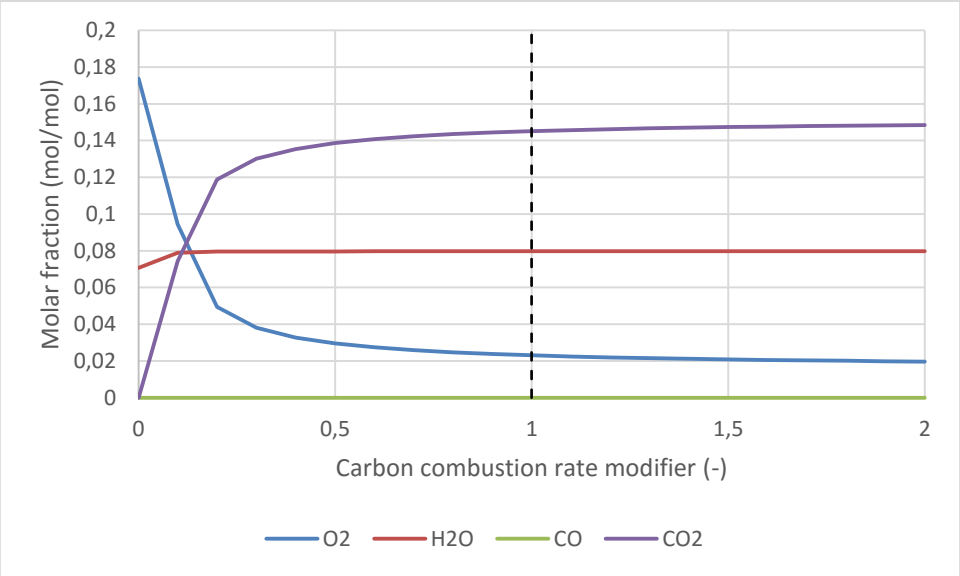

Figure 4.16 – Variation of the outlet gas composition with the carbon combustion rate modifier.

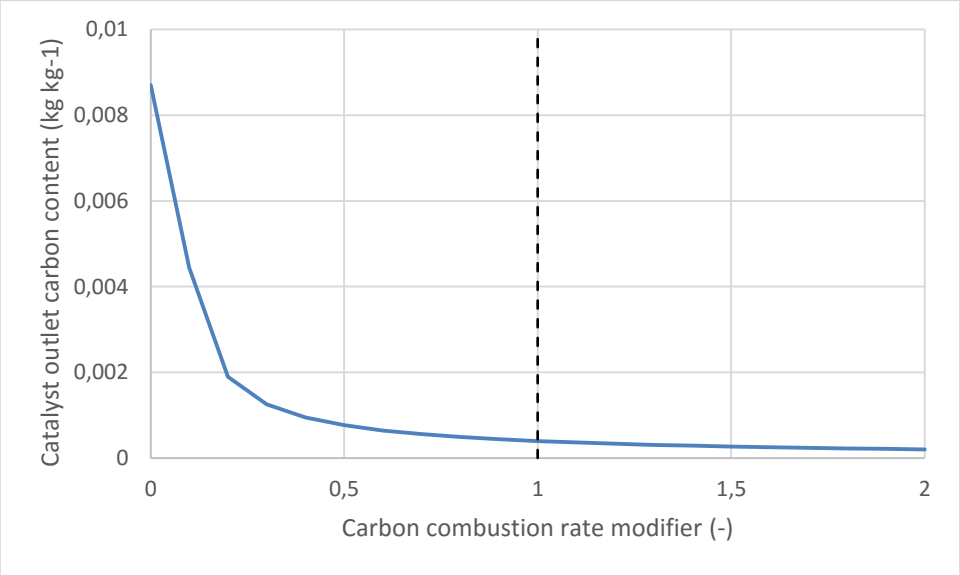

Figure 4.17 – Variation of the carbon content of the catalyst particles at the outlet with the carbon combustion rate modifier.

4.4.3 Hydrogen combustion rate

It is easily verified that the inclusion of the combustion of hydrogen is very important to the model of the regenerator, which some models in the literature choose to ignore. Not including the combustion of hydrogen in the model makes the temperature to drop about 50 K, affecting the combustion rate of the carbon in the coke and altering the results of the simulation.

Others simply consider the combustion of hydrogen to be instantaneous, which these results seem to support: a jump from 0% (no reaction) to 10% of the reaction rate is enough to give almost the same results as 100% of the reaction rate, which suggests that the hydrogen combustion is indeed extremely fast and can be considered instantaneous in a simpler model.

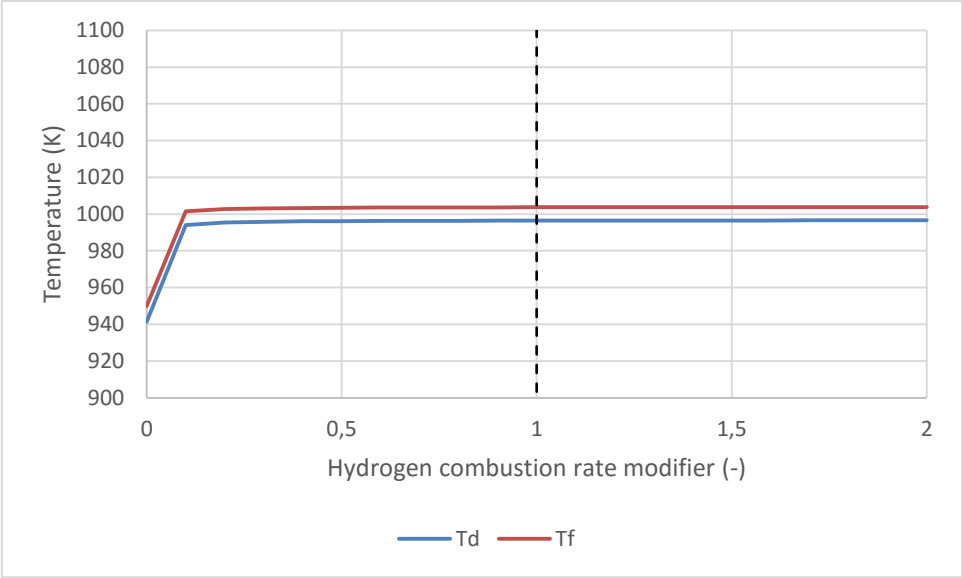

Figure 4.18 – Variation of the average temperature in the dense bed and freeboard with the hydrogen combustion rate modifier.

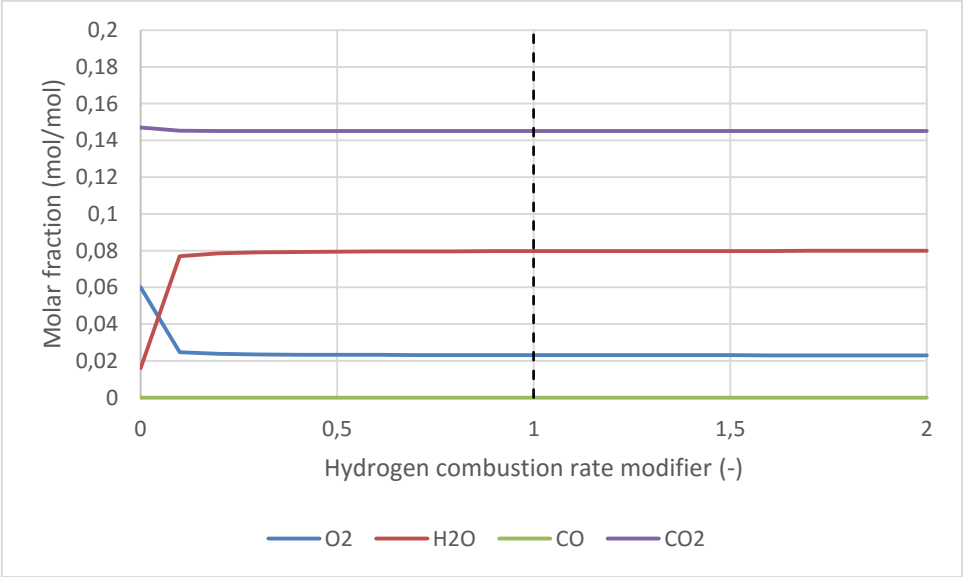

Figure 4.19 – Variation of the outlet gas composition with the hydrogen combustion rate modifier.

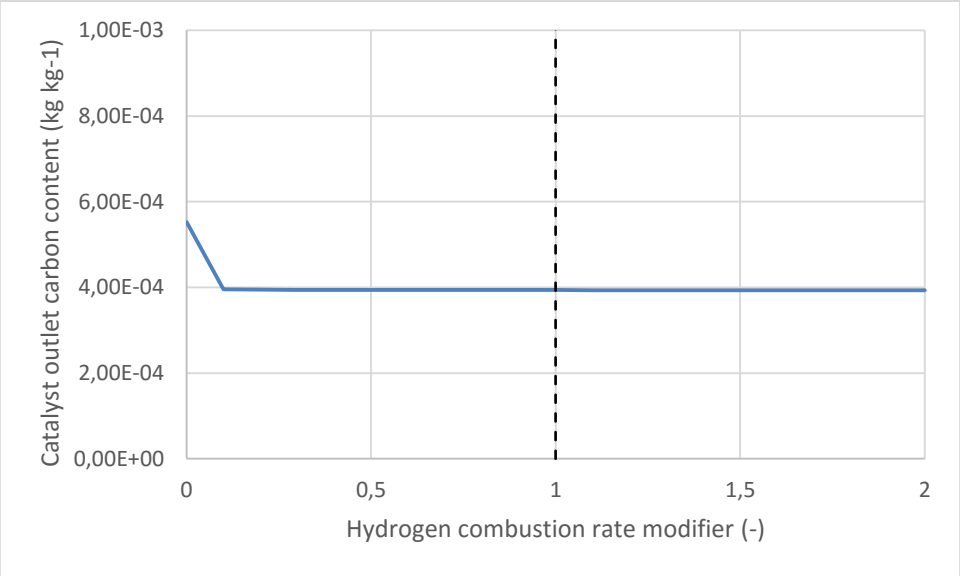

Figure 4.20 – Variation of the carbon content of the catalyst particles at the outlet with the hydrogen combustion rate modifier.

4.4.4 Carbon monoxide combustion rate

In this sensitivity analysis both the homogeneous and heterogeneous combustion of carbon monoxide are affected by the same multiplier.

As can be seen in all plots, the variation in the combustion rate of carbon monoxide has almost no effect in the reactor conditions, since the amount of carbon monoxide in the reactor will always be a very small amount.

As such, a correct reaction rate for the combustion of carbon monoxide is only important to determine its concentration in the reactor and in the outlet combustion gases, and not very important for the overall simulation of the regenerator.

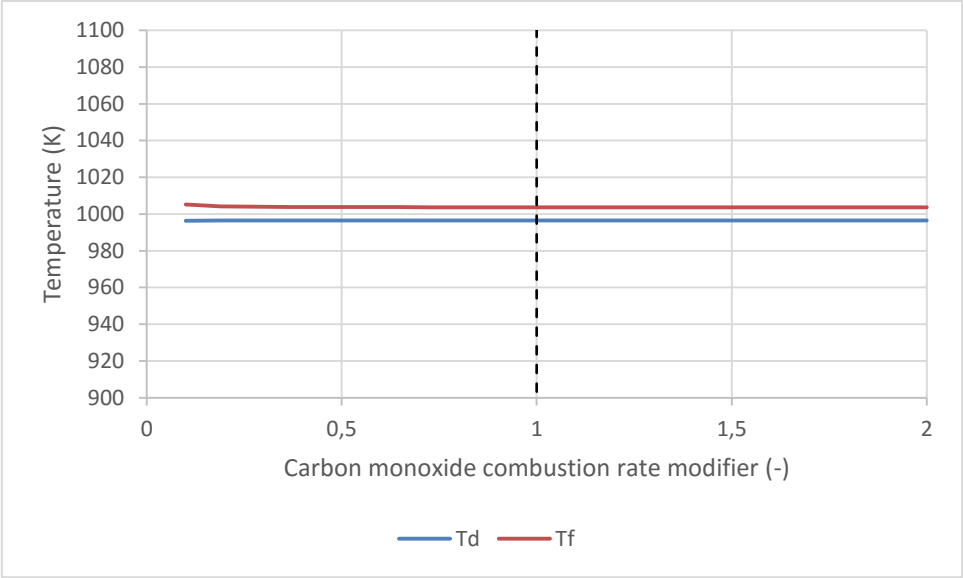

Figure 4.21 – Variation of the average temperature in the dense bed and freeboard with the carbon monoxide combustion rate modifier.

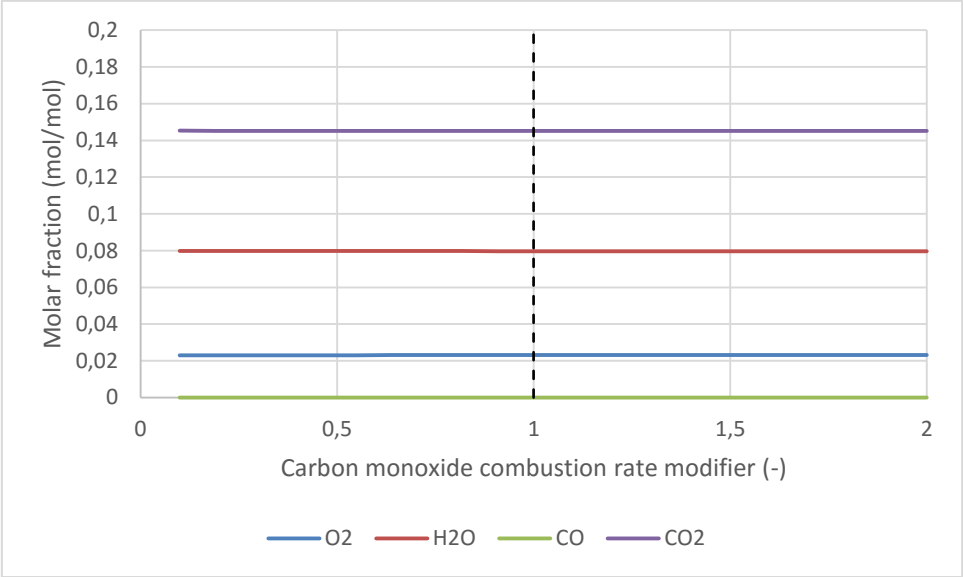

Figure 4.22 – Variation of the outlet gas composition with the carbon monoxide combustion rate modifier.

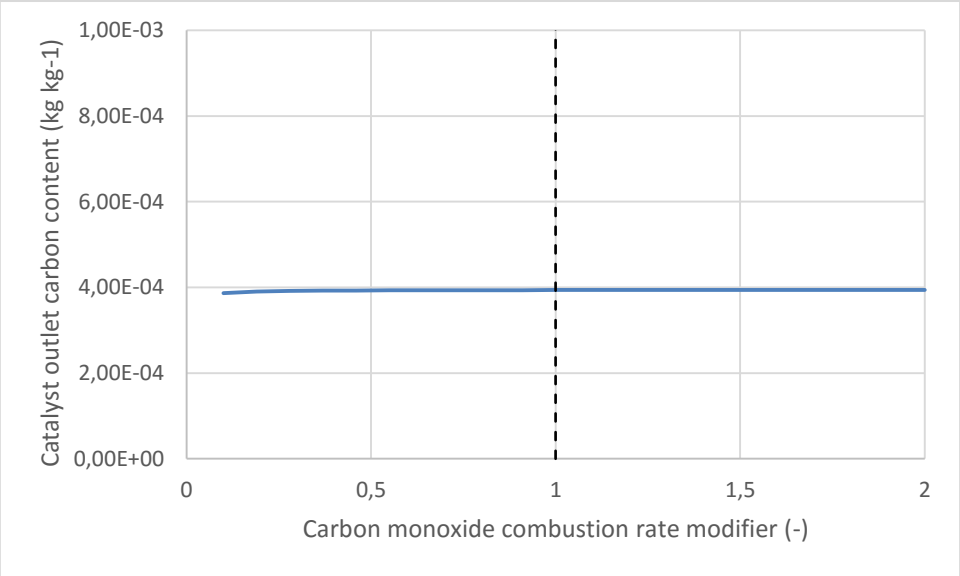

Figure 4.23 – Variation of the carbon content of the catalyst particles at the outlet with the carbon monoxide combustion rate modifier.

4.4.5 Air flowrate

As can be seen in the plots, in the base simulation there is an excess of oxygen (Figure 4.25). Increasing the air flowrate doesn't greatly affect the combustion, as can be seen by the outlet carbon concentration on the catalyst particles (Figure 4.26). However, it causes a dilution effect, increasing the concentration of oxygen and decreasing the concentration of water and carbon dioxide at the regenerator outlet (Figure 4.25). This dilution effect also causes the temperature in the dense bed and in the freeboard to decrease (Figure 4.24). The increase in temperature in the freeboard at higher air flowrates may occur due to a shift in the combustion of carbon monoxide from the dense bed to the freeboard, due to the lower temperatures in the dense bed.

When decreasing the air flowrate, a point is reached where the oxygen becomes the limiting reactant in the combustion reaction and not all of the carbon in the catalyst particles is burnt off, increasing the amount of carbon in the catalyst particles at the regenerator outlet. Because there is a reduced combustion, the temperature also starts decreasing with decreasing air flowrate, after reaching a maximum when the amount of oxygen is neither limiting nor in excess. The amount of carbon dioxide also starts decreasing when air flowrate decreases, because there is less carbon being burnt. The amount of water should remain relatively the same, as the combustion of hydrogen is much faster than the combustion of carbon so it is not very much affected by the decreasing amounts of oxygen, but because there is less nitrogen in the reactor to dilute the combustion gases, the concentration of water keeps increasing.

The air flowrate that enters the regenerator is usually used as a manipulated variable in controlling the regenerator. This sensitivity analysis shows that it is most useful in controlling the regenerator when it works in partial combustion mode, i.e., there isn't enough oxygen to burn off

all of the coke. When in full combustion mode, the air flowrate only affects the temperature of the dense bed, which can also be a variable worth controlling.

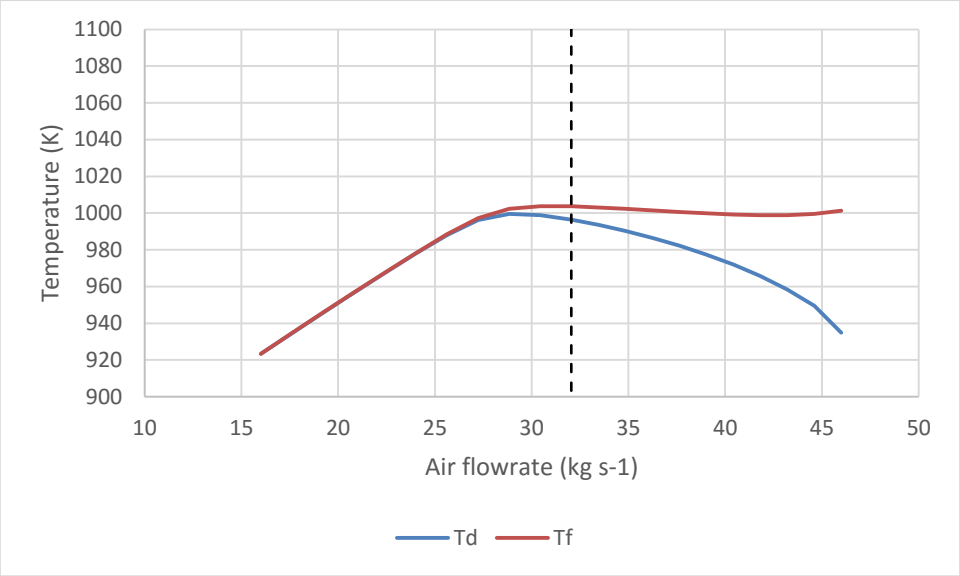

Figure 4.24 – Variation of the average temperature in the dense bed and freeboard with the air flowrate.

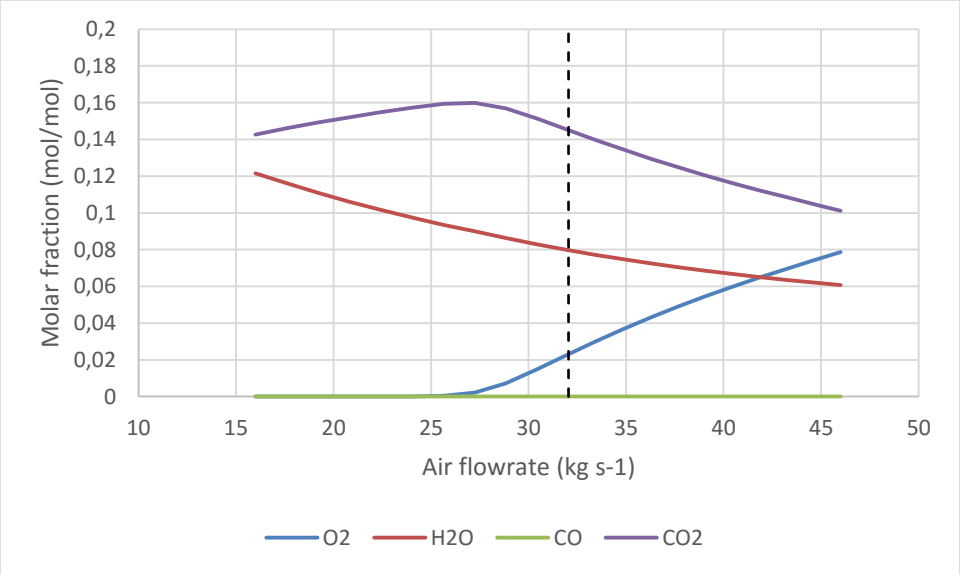

Figure 4.25 – Variation of the outlet gas composition with the air flowrate.

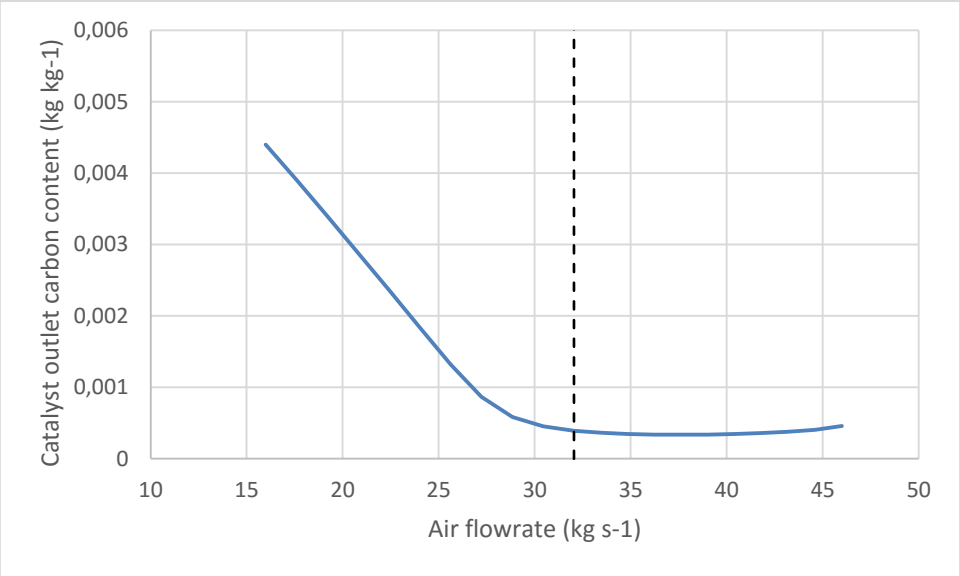

Figure 4.26 – Variation of the carbon content of the catalyst particles at the outlet with the air flowrate.

4.4.6 Catalyst flowrate

Increasing the catalyst flowrate increases the average temperature in both regions of the regenerator for two reasons: more energy enters the regenerator, but more importantly because there is more coke being burnt and releasing energy. Because of the increased combustion, there is more carbon dioxide and water (the combustion reaction products) and less excess oxygen, consumed in the combustion. The outlet catalyst particles carbon content doesn't change significantly because there is still enough oxygen to burn of most of the coke.

If the catalyst flowrate continues increasing, increasing as well the amount of coke that enters the regenerator, it reaches a point where there isn't enough oxygen to burn all of the coke. Oxygen becomes the limiting reactant and the behaviour of the regenerator changes. The carbon content of the catalyst particles at the regenerator outlet starts increasing at a rapid rate, because not all of the coke that enters the regenerator is burnt, and the temperature inside the regenerator starts decreasing, as the catalyst particles now act like a heat sink: the combustion reaction remains the same, releasing the same energy, but now there is more catalyst particles to absorb that heat.

Because the combustion of hydrogen is much faster, the amount of water at the regenerator outlet keeps increasing in these conditions, as the oxygen is consumed first to burn the hydrogen and only the remaining goes to burning the carbon in the coke, which explains why the carbon dioxide amount decreases while the amount of water keeps increasing.

The catalyst flowrate that enters the regenerator is usually used as a manipulated variable to control the regenerator. This sensitivity analysis shows that this variable is capable of affecting the temperature in a way that it can effectively control that variable. However, the control system must be aware that depending on whether the regenerator being operated in full

combustion mode (there is excess oxygen) or partial combustion mode (oxygen is the limiting reactant) the temperature reacts differently to a change in the catalyst flowrate, as can be seen in Figure 4.27: the temperature maximum at approximately 270 kg/s of catalyst represents the transition between these two modes of operation.

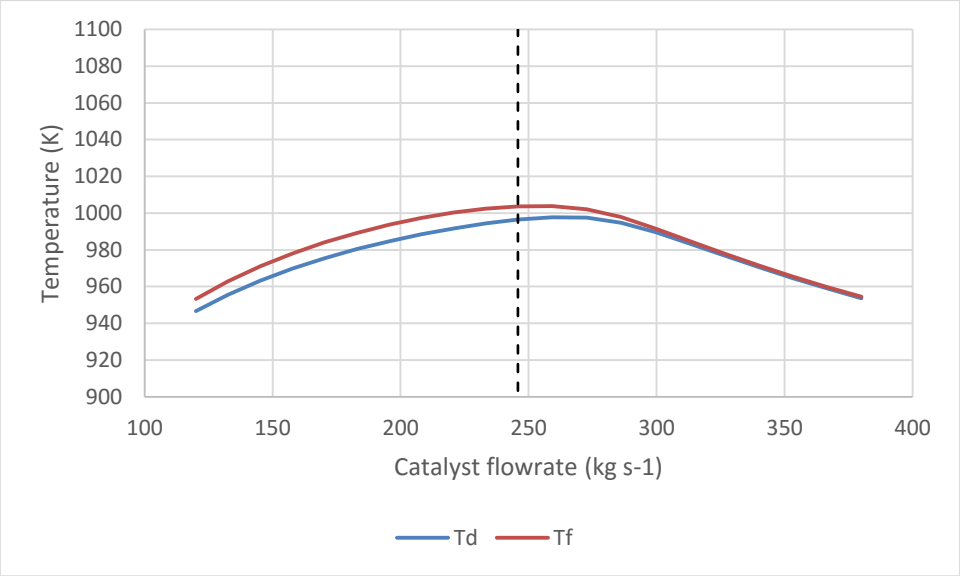

Figure 4.27 – Variation of the average temperature in the dense bed and freeboard with the catalyst flowrate.

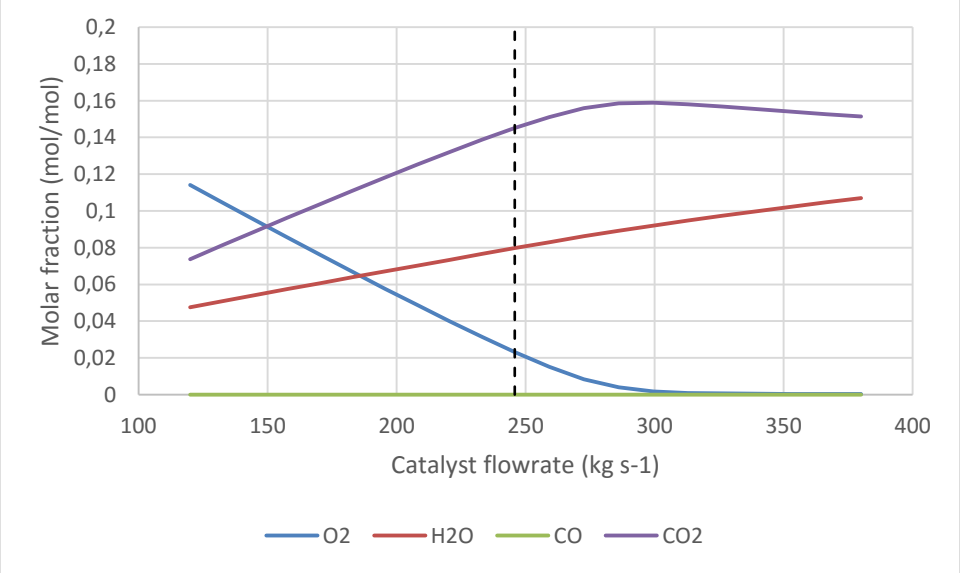

Figure 4.28 – Variation of the outlet gas composition with the catalyst flowrate.

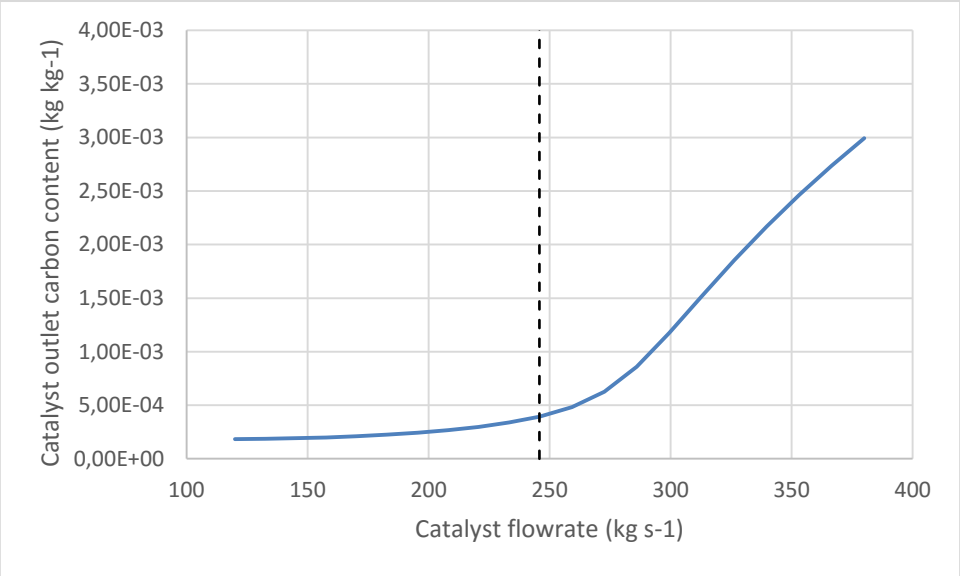

Figure 4.29 – Variation of the carbon content of the catalyst particles at the outlet with the catalyst flowrate.

4.4.7 Catalyst temperature

The catalyst particles temperature has an almost linear effect in the average temperature of the two regenerator regions. Increasing the catalyst particles temperature also increases the temperature in the regenerator.

With the increase in the reactor temperature, the reaction rates also increase, leading to: an increase of the content of the combustion products (water and carbon dioxide) in the combustion gases at the outlet of the regenerator; and a decrease in the oxygen at the regenerator outlet and in the carbon content of the catalyst particles leaving the regenerator.

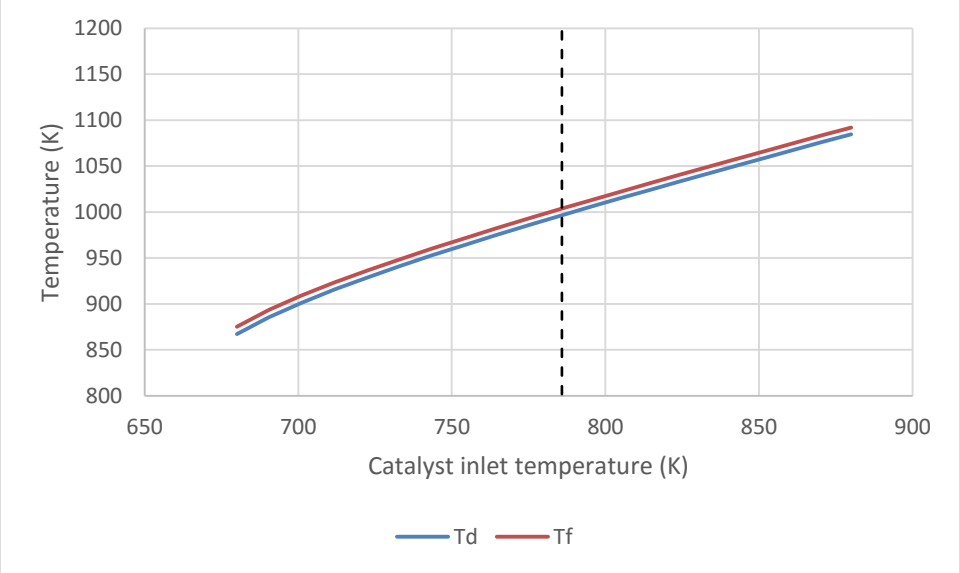

Figure 4.30 – Variation of the average temperature in the dense bed and freeboard with the catalyst inlet temperature.

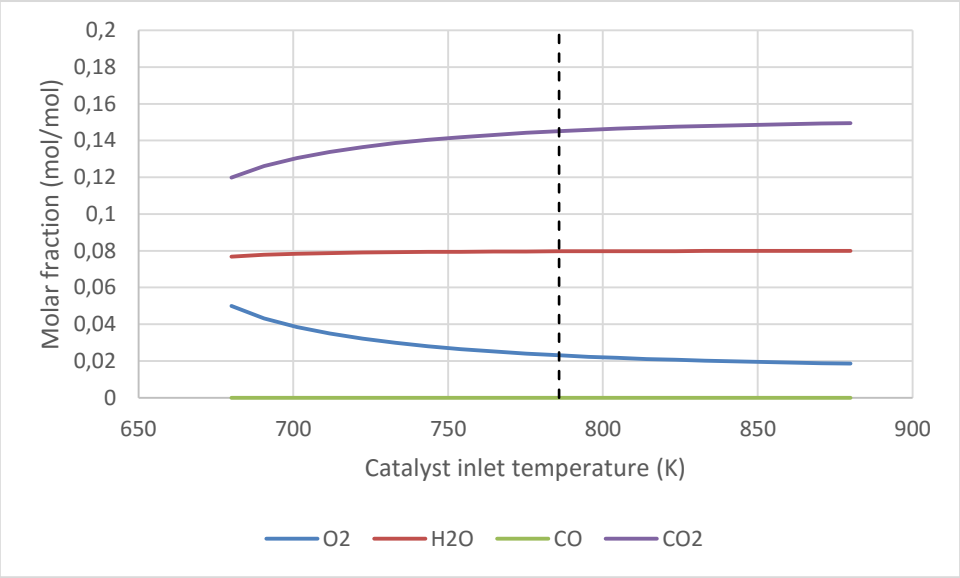

Figure 4.31 – Variation of the outlet gas composition with the catalyst inlet temperature.

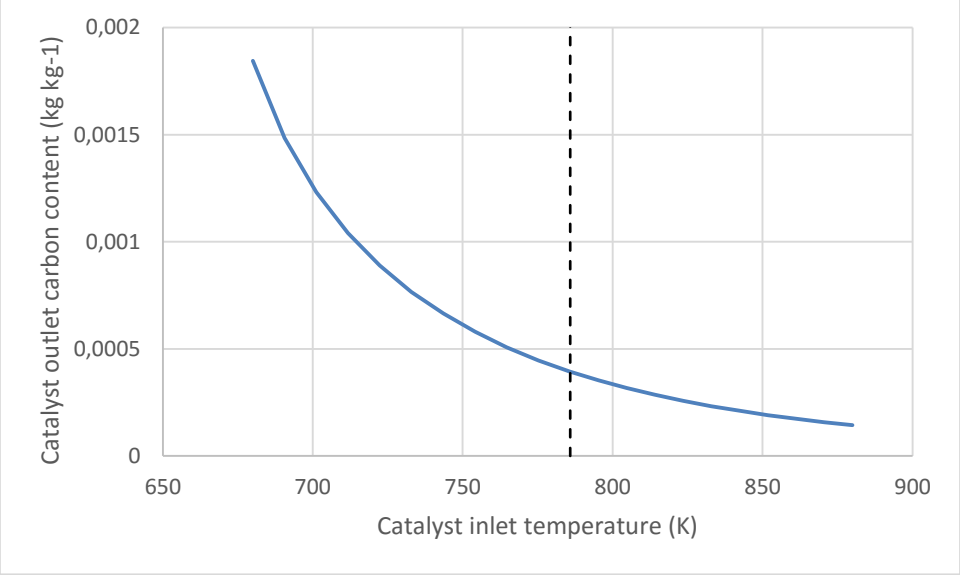

Figure 4.32 – Variation of the carbon content of the catalyst particles at the outlet with the catalyst inlet temperature.

4.4.8 Catalyst inlet carbon content

Increasing the coke concentration makes the average temperature in both regions of the regenerator increase due to the increase of released energy from the combustion. This temperature increase makes the final carbon concentration in the catalyst particles at the outlet decrease, due to the increase in the combustion reactions rates. The increased coke to burn also causes the carbon dioxide and water in the combustion gases increase, as these are the combustion reaction products.

With the increase in combustion, the excess oxygen decreases, up to the point where it becomes the limiting reactant. At this point the outlet carbon concentration increases rapidly, because the excess carbon at the inlet is no longer being burnt. With no more coke being burnt, the temperature in the reactor stabilizes (in the simulation the coke heat capacity is ignored, only the catalyst particles' is considered). Because the combustion of hydrogen is much faster than the combustion of carbon, the water content continues increasing, albeit at a slower rate, and the carbon dioxide content stabilizes, even decreasing a little. This effect can be explained due to the fact that the oxygen reacts preferentially to produce water and more carbon is left in the carbon monoxide form.

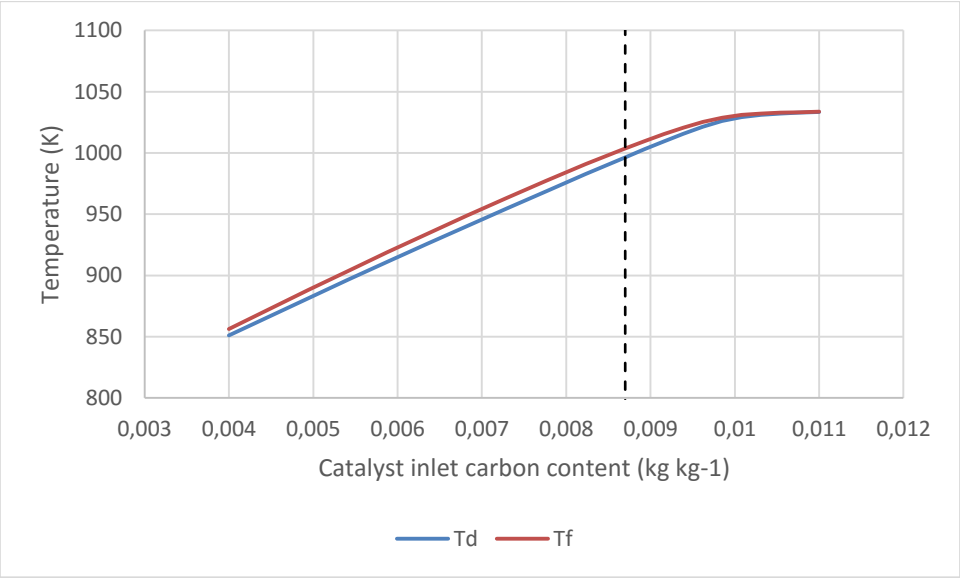

Figure 4.33 – Variation of the average temperature in the dense bed and freeboard with the carbon content of the coke at the inlet.

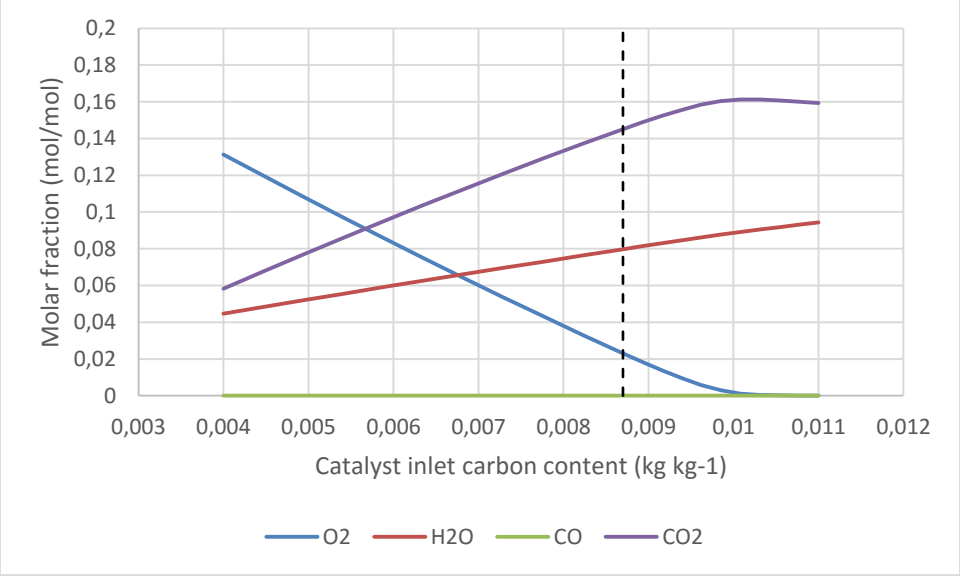

Figure 4.34 – Variation of the outlet gas composition with the carbon content of the coke at the inlet.

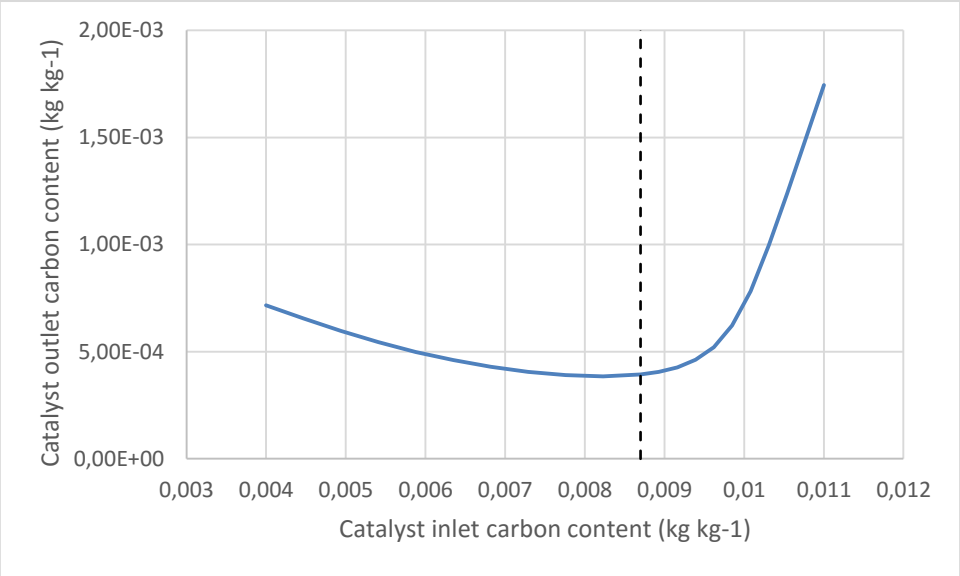

Figure 4.35 – Variation of the carbon content of the catalyst particles at the outlet with the carbon content of the coke at the inlet.

5 Conclusions and Future Work

5.1 Conclusions

A model for the regenerator of a fluid catalytic cracking unit was developed. This model is based on the Generalised Fluidised Bed Reactor (GFBR) model by Abba [33]. The regenerator model developed is significantly more complex and complete than others found in literature.

No reactor profile data for the regenerator were found in literature, either from plant data or from results of other published models. As such, a proper model validation was not possible. However, the simulation results obtained with the regenerator model were analysed anyway and found to be in accordance with the expected results and consistent among themselves.

The two kinetic models tested gave similar results and were in accordance with the available data found in literature. The regenerator model developed in this work with both kinetic models gives good results in terms of the carbon conversion and temperatures inside the regenerator. Comparing with the results found in literature from which the plant data was retrieved, the model developed in this work gives much better results for the carbon conversion with both kinetic models used. After tuning some parameters of the simulation those results were even closer to the plant data available, including the temperatures of the dense bed and freeboard and carbon conversion, with the exception of the concentration of carbon monoxide, which remains very different from the expected value.

A simplification study was performed, where several common assumptions for the regenerator model found in literature were tested. This study showed that the inclusion of dispersion in what would otherwise be a PFR model doesn't affect the overall results of the simulation, although the reactor profiles change.

Even though some conclusions can be drawn from the simplification study, the final results can only be obtained when this regenerator model is connected to a riser model, completing the model of a FCCU. As the purpose of the regenerator model developed in this work is to be part of a modular library of FCC models, the validation of the regenerator model can only be concluded when the FCCU model is completed. This also applies to using a model that considers different fluidisation regimes instead of having it assumed from the beginning. A comparison with other regenerator models in a complete model of FCC is required.

A sensitivity analysis was also performed on a number of key variables. The most important results from this analysis are: the catalyst flowrate and the air flowrate are confirmed to be good manipulated variables for controlling the regenerator; the kinetics of carbon monoxide combustion does not have a significant influence on the regenerator, with neither temperatures or carbon conversion altering significantly; and the inclusion of hydrogen combustion is important when simulating the regenerator as it affects greatly the results of the simulation, but can be considered instantaneous, instead of explicitly modelling its combustion, further simplifying the model, due to the very high combustion rate.

Overall, the objectives of this work were achieved, with the limitations stated above.

5.2 Future work

This regenerator model is only the start of what could be a very big project: the creation of a library of FCC models, which can be used to model and simulate a FCCU integrated in a complete process plant.

As such, future work could include the development of the remaining FCCU models, most notably the riser, and also developing a dynamic version of those models, to simulate the transient response of the FCC plant, which is very important for studying and optimising the advanced control of FCC units.

The regenerator model also needs to be validated against real plant data. Although a limited validation was possible in this work, profile data are still required to properly validate the regenerator model.

A simplified model of the regenerator should be implemented in order to properly compare the regenerator model developed in this work with models that assume a CSTR model for one of its phases. Such comparison would support a decision on whether the complex model developed in this work is necessary or if the detail that it provides when compared to other models found in literature is not required for specific model applications.

6 References

[1] R. Sadeghbeigi, *Fluid Catalytic Cracking Handbook*. 2012.

[2] P. K. Niccum and C. R. Santner, “KBR Fluid Catalytic Cracking Process,” in *Handbook of petroleum refining processes*, Third Edit., R. A. Meyers, Ed. McGraw-Hill Professional, 2004, pp. 3.3 – 3.34.

[3] J. de L. R. Fernandes, “Nonlinear modelling of industrial fluid catalytic cracking processes for model-based-control and optimization studies,” UTL, Instituto Superior T�cnico, Lisboa, 2007.

[4] C. L. Hemler and L. F. Smith, “UOP Fluid Catalytic Cracking Process,” in *Handbook of petroleum refining processes*, R. A. Meyers, Ed. McGraw-Hill Professional, 2004, pp. 3.47 – 3.69.

[5] O. Faltsi-Saravelou, I. A. Vasalos, and G. Dimogiorgas, “FBSim: A model for fluidized bed simulation—II. Simulation of an industrial fluidized catalytic cracking regenerator,” *Comput. Chem. Eng.*, vol. 15, no. 9, pp. 647–656, Sep. 1991.

[6] W. S. Letzsch, “Stone & Webster–Institut Français Du Pétrole Fluid RFCC Process,” in *Handbook of petroleum refining processes*, Third Edit., R. A. Meyers, Ed. McGraw-Hill Professional, 2004, pp. 3.71 – 3.94.

[7] C. I. C. Pinheiro, J. L. Fernandes, L. Domingues, A. J. S. Chambel, I. Graça, N. M. C. Oliveira, H. S. Cerqueira, and F. R. Ribeiro, “Fluid Catalytic Cracking (FCC) Process Modeling, Simulation, and Control,” *Ind. Eng. Chem. Res.*, vol. 51, no. 1, pp. 1–29, Jan. 2012.

[8] S. Raseev, *Thermal and Catalytic Processes in Petroleum Refining*. Mercel Dekker, Inc., 2003.

[9] K. Leclère, C. Briens, T. Gauthier, J. Bayle, P. Guigon, and M. Bergougnou, “Experimental measurement of droplet vaporization kinetics in a fluidized bed,” *Chem. Eng. Process. Process Intensif.*, vol. 43, no. 6, pp. 693–699, 2004.

[10] S. Kumar, A. Chadha, R. Gupta, and R. Sharma, “CATCRAK: A Process Simulator for an Integrated FCC-Regenerator System,” *Ind. Eng. Chem. Res.*, vol. 34, no. 11, pp. 3737–3748, Nov. 1995.

[11] P. K. Dasila, I. Choudhury, D. Saraf, S. Chopra, and A. Dalai, “Parametric Sensitivity Studies in a Commercial FCC Unit,” *Adv. Chem. Eng. Sci.*, vol. 2, no. 1, pp. 136–149, 20112.

[12] H. Ali and S. Rohani, “Dynamic modeling and simulation of a riser-type fluid catalytic cracking unit,” *Chem. Eng. Technol.*, vol. 20, no. 2, pp. 118–130, 1997.

[13] A. Gupta and D. Subba Rao, “Effect of feed atomization on FCC performance: simulation of entire unit,” *Chem. Eng. Sci.*, vol. 58, no. 20, pp. 4567–4579, 2003.

[14] A. Gupta and D. Subba Rao, “Model for the performance of a fluid catalytic cracking

(FCC) riser reactor: effect of feed atomization," *Chem. Eng. Sci.*, vol. 56, no. 15, pp. 4489–4503, 2001.

[15] R. K. Gupta, V. Kumar, and V. K. Srivastavaa, "Modelling of Fluid Catalytic Cracking Riser Reactor: A Review," *Int. J. Chem. React. Eng.*, vol. 8, no. 1, 2010.

[16] S. V. Nayak, S. L. Joshi, and V. V. Ranade, "Modeling of vaporization and cracking of liquid oil injected in a gas–solid riser," *Chem. Eng. Sci.*, vol. 60, no. 22, pp. 6049–6066, 2005.

[17] A. Neri and D. Gidaspow, "Riser hydrodynamics: Simulation using kinetic theory," *AIChE J.*, vol. 46, no. 1, pp. 52–67, 2000.

[18] H. C. Alvarez-Castro, E. M. Matos, M. Mori, W. Martignoni, and R. Ocone, "The influence of the fluidization velocities on products yield and catalyst residence time in industrial risers," *Adv. Powder Technol.*, vol. 26, no. 3, pp. 836–847, 2015.

[19] W. Shuai, L. Huilin, L. Guodong, S. Zhiheng, X. Pengfei, and D. Gidaspow, "Modeling of cluster structure-dependent drag with Eulerian approach for circulating fluidized beds," *Powder Technol.*, vol. 208, no. 1, pp. 98–110, 2011.

[20] M. T. Shah, R. P. Utikar, M. O. Tade, V. K. Pareek, and G. M. Evans, "Simulation of gas–solid flows in riser using energy minimization multiscale model: Effect of cluster diameter correlation," *Chem. Eng. Sci.*, vol. 66, no. 14, pp. 3291–3300, 2011.

[21] S. Benyahia, H. Arastoopour, T. M. Knowlton, and H. Massah, "Simulation of particles and gas flow behavior in the riser section of a circulating fluidized bed using the kinetic theory approach for the particulate phase," *Powder Technol.*, vol. 112, no. 1, pp. 24–33, 2000.

[22] H. Sabbaghan, R. Sotudeh-Gharebagh, and N. Mostoufi, "Modeling the acceleration zone in the riser of circulating fluidized beds," *Powder Technol.*, vol. 142, no. 2, pp. 129–135, 2004.

[23] G. M. Bollas, A. A. Lappas, D. K. Iatridis, and I. A. Vasalos, "Five-lump kinetic model with selective catalyst deactivation for the prediction of the product selectivity in the fluid catalytic cracking process," *Catal. Today*, vol. 127, no. 1, pp. 31–43, 2007.

[24] P. Cristina, "Four – Lump Kinetic Model vs. Three - Lump Kinetic Model for the Fluid Catalytic Cracking Riser Reactor," *Procedia Eng.*, vol. 100, pp. 602–608, 2015.

[25] M. A. Abul-Hamayel, M. A.-B. Siddiqui, T. Ino, and A. M. Aitani, "Experimental determination of high-severity fluidized catalytic cracking (HS-FCC) deactivation constant," *Appl. Catal. A Gen.*, vol. 237, no. 1, pp. 71–80, 2002.

[26] C. Derouin, D. Nevicato, M. Forissier, G. Wild, and J.-R. Bernard, "Hydrodynamics of Riser Units and Their Impact on FCC Operation," *Ind. Eng. Chem. Res.*, vol. 36, no. 11, pp. 4504–4515, Nov. 1997.

[27] S. M. Jacob, B. Gross, S. E. Voltz, and V. W. Weekman, "A lumping and reaction scheme for catalytic cracking," *AIChE J.*, vol. 22, no. 4, pp. 701–713, 1976.

[28] R. Quintana-Solórzano, J. W. Thybaut, P. Galtier, and G. B. Marin, “Simulation of an industrial riser for catalytic cracking in the presence of coking using Single-Event MicroKinetics,” *Catal. Today*, vol. 150, no. 3, pp. 319–331, 2010.

[29] R. J. Quann and S. B. Jaffe, “Building useful models of complex reaction systems in petroleum refining,” *Chem. Eng. Sci.*, vol. 51, no. 10, pp. 1615–1635, May 1996.

[30] C. I. C. Pinheiro, F. Lemos, and F. Ramôa Ribeiro, “Dynamic modelling and network simulation of n-heptane catalytic cracking: influence of kinetic parameters,” *Chem. Eng. Sci.*, vol. 54, no. 11, pp. 1735–1750, Jun. 1999.

[31] J. Zhang, Z. Wang, H. Jiang, J. Chu, J. Zhou, and S. Shao, “Modeling fluid catalytic cracking risers with special pseudo-components,” *Chem. Eng. Sci.*, vol. 102, pp. 87–98, 2013.

[32] J. Corella, “On the Modeling of the Kinetics of the Selective Deactivation of Catalysts. Application to the Fluidized Catalytic Cracking Process,” *Ind. Eng. Chem. Res.*, vol. 43, no. 15, pp. 4080–4086, Jul. 2004.

[33] I. Abba, “A generalized fluidized bed reactor model across the flow regimes,” The University of British Columbia, 2001.

[34] M. L. Thompson, H. Bi, and J. R. Grace, “A generalized bubbling/turbulent fluidized-bed reactor model,” *Chem. Eng. Sci.*, vol. 54, no. 13–14, pp. 2175–2185, Jul. 1999.

[35] D. Kunii and O. Levenspiel, “Fluidized reactor models. 1. For bubbling beds of fine, intermediate, and large particles. 2. For the lean phase: freeboard and fast fluidization,” *Ind. Eng. Chem. Res.*, vol. 29, no. 7, pp. 1226–1234, Jul. 1990.

[36] I. A. Abba, J. R. Grace, and H. T. Bi, “Variable-gas-density fluidized bed reactor model for catalytic processes,” *Chem. Eng. Sci.*, vol. 57, no. 22, pp. 4797–4807, 2002.

[37] I. A. Abba, J. R. Grace, H. T. Bi, and M. L. Thompson, “Spanning the flow regimes: Generic fluidized-bed reactor model,” *AIChE J.*, vol. 49, no. 7, pp. 1838–1848, Jul. 2003.

[38] *gPROMS ProcessBuilder Documentation*, Release 1. Process System Enterprise, 2015.

[39] A. Mahecha-Botero, J. R. Grace, S. S. E. H. Elnashaie, and C. J. Lim, “ADVANCES IN MODELING OF FLUIDIZED-BED CATALYTIC REACTORS: A COMPREHENSIVE REVIEW,” *Chem. Eng. Commun.*, vol. 196, no. 11, pp. 1375–1405, Jul. 2009.

[40] S. M. Al-Zahrani, A. M. Aljodai, and K. M. Wagialla, “Modelling and simulation of 1,2-dichloroethane production by ethylene oxychlorination in fluidized-bed reactor,” *Chem. Eng. Sci.*, vol. 56, no. 2, pp. 621–626, 2001.

[41] J. C. S. Moreira and C. A. M. Pires, “Modelling and simulation of an oxychlorination reactor in a fluidized bed,” *Can. J. Chem. Eng.*, vol. 88, no. 3, pp. 350–358, 2010.

[42] K. . Lim, J. . Zhu, and J. . Grace, “Hydrodynamics of gas-solid fluidization,” *Int. J. Multiph. Flow*, vol. 21, pp. 141–193, Dec. 1995.

[43] O. Faltsi-Saravelou and I. A. Vasalos, “FBSim: A model for fluidized bed simulation—I. Dynamic modeling of an adiabatic reacting system of small gas fluidized particles,”

Comput. Chem. Eng., vol. 15, no. 9, pp. 639–646, Sep. 1991.

[44] A. R. Secchi, M. G. Santos, G. A. Neumann, and J. O. Trierweiler, “A dynamic model for a FCC UOP stacked converter unit,” *Comput. Chem. Eng.*, vol. 25, no. 4, pp. 851–858, 2001.

[45] I.-S. Han and C.-B. Chung, “Dynamic modeling and simulation of a fluidized catalytic cracking process. Part I: Process modeling,” *Chem. Eng. Sci.*, vol. 56, no. 5, pp. 1951–1971, 2001.

[46] I.-S. Han and C.-B. Chung, “Dynamic modeling and simulation of a fluidized catalytic cracking process. Part II: Property estimation and simulation,” *Chem. Eng. Sci.*, vol. 56, no. 5, pp. 1973–1990, 2001.